Journal of Sound and Vibration 329 (2010) 3280–3303

Contents lists available at ScienceDirect

Journal of Sound and Vibration

journal homepage: www.elsevier.com/locate/jsvi

The influence of cross-order terms in interface mobilities for structure-borne sound source characterization

H.A. Bonhoff *, B.A.T. Petersson

Institute of Fluid Mechanics and Engineering Acoustics, Technische Universität Berlin, Einsteinufer 25, 10587 Berlin, Germany

ARTICLE INFO

Article history:
Received 17 February 2009
Received in revised form
15 February 2010
Accepted 15 February 2010
Handling Editor: D.J. Thompson
Available online 19 March 2010

ABSTRACT

For the characterization of structure-borne sound sources with multi-point or continuous interfaces, substantial simplifications and physical insight can be obtained by incorporating the concept of interface mobilities. The applicability of interface mobilities, however, relies upon the admissibility of neglecting the so-called cross-order terms. Hence, the objective of the present paper is to clarify the importance and significance of cross-order terms for the characterization of vibrational sources. From previous studies, four conditions have been identified for which the cross-order terms can become more influential. Such are non-circular interface geometries, structures with distinctively differing transfer paths as well as a suppression of the zero-order motion and cases where the contact forces are either in phase or out of phase. In a theoretical study, the former four conditions are investigated regarding the frequency range and magnitude of a possible strengthening of the cross-order terms. For an experimental analysis, two source–receiver installations are selected, suitably designed to obtain strong cross-order terms. The transmitted power and the source descriptors are predicted by the approximations of the interface mobility approach and compared with the complete calculations. Neglecting the cross-order terms can result in large misinterpretations at certain frequencies. On average, however, the cross-order terms are found to be insignificant and can be neglected with good approximation. The general applicability of interface mobilities for structure-borne sound source characterization and the description of the transmission process thereby is confirmed.

1. Introduction

For the design of vibrational sources and optimization of the transmitted power, an approach for structure-borne sound source characterization is required, which provides the engineer with physical insight and absolute source data. The vibration amplitude at the source–receiver interface and the active power fed to the receiver constitute the central quantities required and can be obtained from the complex power Q [1]. Derived from the definition of complex power and being independent of the receiver properties, see Eq. (1), the source descriptor S [2] forms a consistent basis for studies of vibrational sources:

$$Q = S \cdot C_f, \quad S = \frac{1}{2}\frac{|v_{FS}|^2}{Y_S^*}, \quad C_f = \frac{Y_S^* Y_R}{|Y_S + Y_R|^2} \tag{1}$$

A list of symbols is given in the nomenclature.

* Corresponding author. Tel.: +49 30 31428996; fax: +49 30 31425135.
E-mail address: hannes.bonhoff@tu-berlin.de (H.A. Bonhoff).

0022-460X/$ - see front matter © 2010 Elsevier Ltd. All rights reserved.
doi:10.1016/j.jsv.2010.02.020

Nomenclature

Symbols

C	interface circumference
C_f	coupling function
d	shortest distance along the structure between excitation and response positions
f	frequency
F	force distribution
$\hat{F}$	force amplitude
$\hat{F}_q$	force order
I_{xx}, I_{yy}	moments of inertia
j	complex number
k_B	bending wavenumber
k_p, k_q	interface numbers
L_0	half the diagonal of the rectangular interface
m	mass
p, q	order numbers
Q	complex power
r_0	interface radius
Δs	shortest distance along the interface between excitation and response positions
s	response interface coordinate
s_0	excitation interface coordinate
S	source descriptor
S_p	source descriptor order
v	velocity
$\hat{v}_p$	velocity order
W	transmitted power
Y	mobility
$\hat{Y}_{pq}$	interface mobility
$\hat{Y}_{p-p}$	equal-order interface mobility
Y_{vF}^{∞}	point mobility of an infinite plate
ω	angular frequency

Indices

approx	equal-order approximation
BS	blocked source
FS	freely suspended source
L	lowest value
R	receiver
S	source
U	highest value

Initially, the concept of source descriptor and coupling function is valid for the single-point and single-component case only. By reformulating the source descriptor concept in terms of interface mobilities [3], source–receiver assemblies with multi-point or continuous connections, see Fig. 1, can be investigated. The interface mobility approach offers a scheme where the physical source is subdivided into a series of theoretical source orders. Such orders are directly linked to elementary vibrational characteristics such as the rigid-body motion and consequently represent physically highly comprehensible quantities. However, the applicability of the interface mobility approach critically depends on the admissibility of neglecting the coupling between different orders. If such a cross-order coupling is shown to be negligible, each order can be treated as a single-point and single-component system. The thereby gained formal simplicity of the interface mobility approach in combination with the physical insight is essential for planning and low-noise design. The so-called cross-order terms describe the coupling between different orders and consist of cross-order interface mobilities and force orders.

The influence of cross-order interface mobilities has been studied for two generic types of structures, see Refs. [3,4], and an investigation of the distribution of the force-orders is presented in Ref. [5]. Based on the knowledge of the cross-order interface mobilities and the force orders, the significance of the complete cross-order terms is investigated in the present work. Four conditions that can possibly lead to a strengthening of the cross-order terms are examined from a theoretical and an experimental point of view. Whilst it is recognized that moment excitation can be significant [6], the analysis presented here is confined to forces perpendicular to the structure. In analogy with the description of a moment excitation by means of two point forces that are acting out of phase, however, a generalization of the results is expected to be possible.

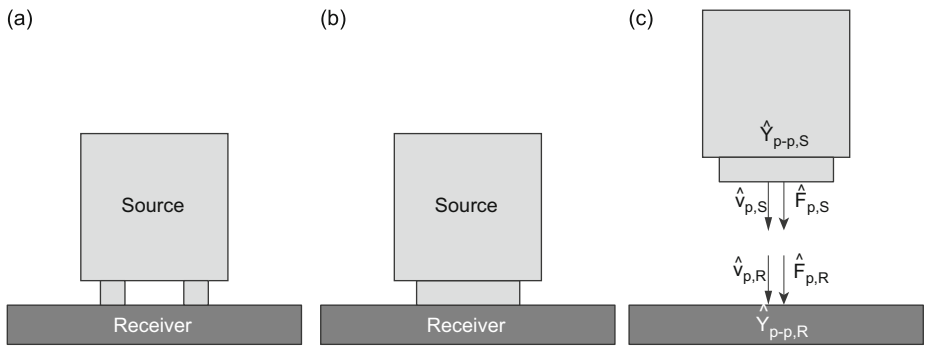

Fig. 1. Schematic illustration of source–receiver installations: (a) multi-point installation; (b) continuous installation; (c) notation of the field variables.

In Section 2, the concept of interface mobilities is outlined with a derivation of the source descriptor for vibrational sources with a multi-point or continuous connection to the receiver. A short survey is given of the previous publications in the series, i.e. Refs. [3–5], from which the conditions that can possibly lead to a strengthening of the cross-order terms are deduced. The effect of a non-circular interface geometry on the significance of the cross-order terms is studied in Section 3, followed by an analysis of structures with distinctively differing transfer paths, see Section 4. Section 5 deals with a possible suppression of the in-phase motion along the interface and a deterministic phase of the contact forces is investigated in Section 6. In accordance with such four conditions, two potentially critical source–receiver installations are designed and examined in an experimental comparison in Section 7.

2. Interface mobility approach

For multi-point connections between sources and receivers, a single continuous interface can be formed, which passes all contact points, see Fig. 2(a). Consequently, the field variables, e.g. forces and velocities, can be treated as continuous and strictly periodic along the interface. The latter is evident for a continuous connection between a source and a receiver, see Fig. 2(b). By means of a spatial Fourier decomposition, the velocity $v(s)$ can be described in terms of its interface orders $\hat{v}_p$,

$$\hat{v}_p = \frac{1}{C}\int_0^C v(s)\mathrm{e}^{-\mathrm{j}k_p s}\,\mathrm{d}s, \quad v(s) = \sum_{p=-\infty}^{\infty} \hat{v}_p \mathrm{e}^{\mathrm{j}k_p s}, \quad k_p = \frac{2p\pi}{C},\ p \in \mathbb{Z}. \tag{2}$$

Similarly, the force orders are obtained by

$$\hat{F}_q = \frac{1}{C}\int_0^C F(s_0)\mathrm{e}^{-\mathrm{j}k_q s_0}\,\mathrm{d}s_0, \quad F(s_0) = \sum_{q=-\infty}^{\infty} \hat{F}_q \mathrm{e}^{\mathrm{j}k_q s_0}, \quad k_q = \frac{2q\pi}{C},\ q \in \mathbb{Z}. \tag{3}$$

In Fig. 3, a few interface orders are plotted along a circular interface. They could be either force or velocity orders. When summing up a truncated series of such interface orders with the corresponding complex amplitudes $\hat{v}_p$ or $\hat{F}_q$, the initial spatial velocity or force distribution is approximated, see Eq. (2) or (3), respectively.

By similarly expanding the point and transfer mobilities, the interface mobilities can be written as

$$\hat{Y}_{pq} = \frac{1}{C^2}\int_0^C \int_0^C Y(s|s_0)\mathrm{e}^{-\mathrm{j}k_p s}\mathrm{e}^{-\mathrm{j}k_q s_0}\,\mathrm{d}s\,\mathrm{d}s_0, \quad Y(s|s_0) = \sum_{p=-\infty}^{\infty}\sum_{q=-\infty}^{\infty} \hat{Y}_{pq}\mathrm{e}^{\mathrm{j}k_p s}\mathrm{e}^{\mathrm{j}k_q s_0}. \tag{4}$$

Analogous to the shape of interface orders, see Fig. 3, the shape functions of interface mobilities can be visualized as shown in Figs. 4 and 5, cf. [3]. The interface mobility shape functions can be interpreted as components of the shape function of

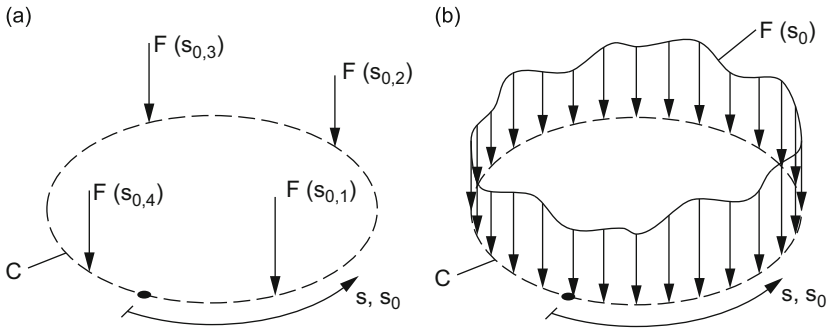

Fig. 2. Illustration of source–receiver interfaces: (a) multi-point interface; (b) continuous interface. – – – interface.

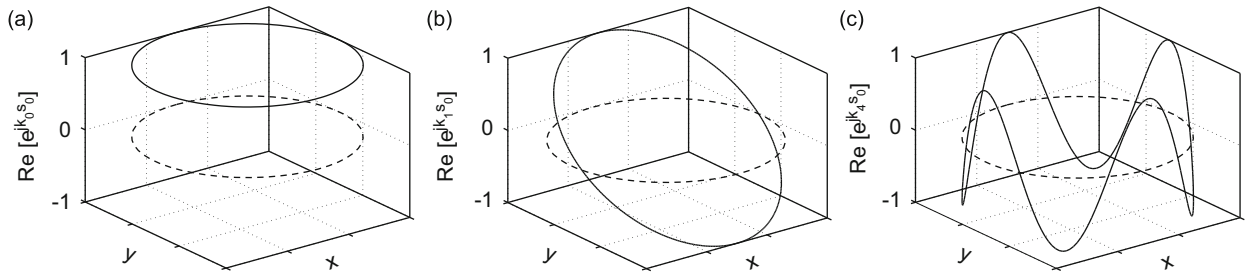

Fig. 3. Illustration of interface order distributions along a circular interface: (a) zero order; (b) first order; (c) fourth order. — interface order; – – – interface.

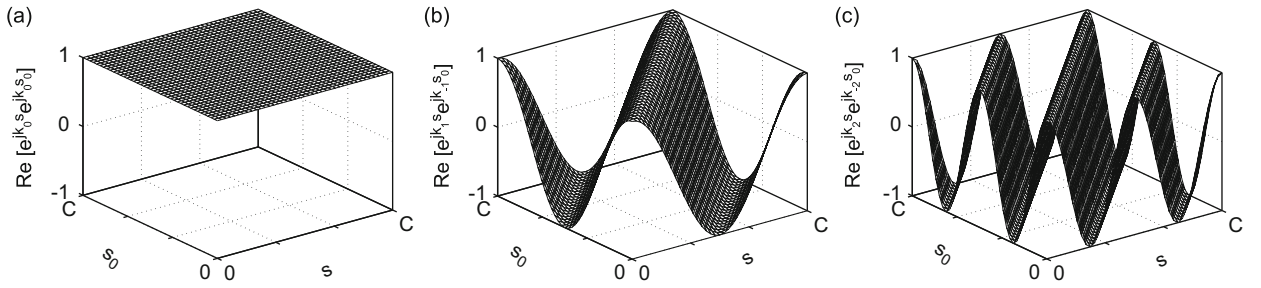

Fig. 4. Illustration of equal-order interface mobility shape functions: (a) $\hat{Y}_{00}$; (b) $\hat{Y}_{1-1}$; (c) $\hat{Y}_{2-2}$.

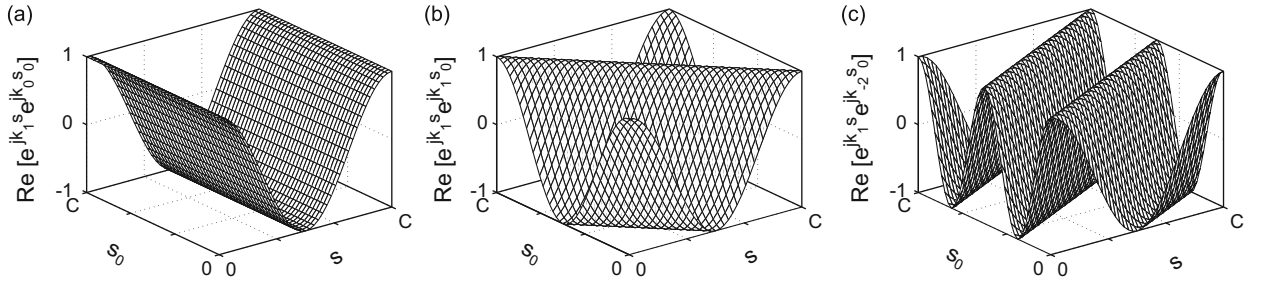

Fig. 5. Illustration of cross-order interface mobility shape functions: (a) $\hat{Y}_{10}$; (b) $\hat{Y}_{11}$; (c) $\hat{Y}_{1-2}$.

$Y(s|s_0)$, i.e. the ordinary mobility shape function, for an arbitrary line interface on any kind of structure. In the ordinary mobility shape functions, the point mobilities are found on the main diagonal, where s equals s_0, and the transfer mobilities are found on the off-diagonal elements. Considering the real part of the mobility shape functions facilitates the physical interpretation. For a unity excitation force at s_0, the ordinary mobility shape function represents the instantaneous vibration amplitudes of the structure along the interface.

In the spatial domain, a velocity at a certain point consists of a superposition of the contributions of all forces acting on the structure. Analogously, a velocity order is composed of a sum of the contributions of all force orders [3],

$$\hat{v}_p = C \sum_{q=-\infty}^{\infty} \hat{Y}_{p-q}\hat{F}_q = C\hat{Y}_{p-p}\hat{F}_p + C \sum_{\substack{q=-\infty \\ q\neq p}}^{\infty} \hat{Y}_{p-q}\hat{F}_q. \tag{5}$$

As indicated, the sum in Eq. (5) can be divided into two parts, i.e. the contribution of a force of the same order $\hat{F}_p$ coupled through the interface mobility $\hat{Y}_{p-p}$ and the contribution of all other force orders, $\hat{Y}_{p-q}\hat{F}_q$ with $p \neq q$. The first part is termed the equal-order term and includes the equal-order interface mobility $\hat{Y}_{p-p}$. The second part comprises all cross-order terms with the cross-order interface mobilities.

The complex power in terms of interface mobilities is given by [3]

$$Q = \frac{C^2}{2} \sum_{p=-\infty}^{\infty} \sum_{q=-\infty}^{\infty} \hat{F}^*_{p,R}\hat{Y}_{p-q,R}\hat{F}_{q,R} = \frac{C^2}{2} \sum_{p=-\infty}^{\infty} \hat{Y}_{p-p,R}|\hat{F}_{p,R}|^2 + \frac{C^2}{2} \sum_{p=-\infty}^{\infty} \sum_{\substack{q=-\infty \\ q\neq p}}^{\infty} \hat{F}^*_{p,R}\hat{Y}_{p-q,R}\hat{F}_{q,R}. \tag{6}$$

For structure-borne sound source characterization using the source descriptor and coupling function, the complex power has to be based on the free velocity of the source v_{FS}, see Eq. (1). When deriving the complex power based on the free source velocity in terms of interface mobilities, the cross-order terms have to be neglected in the following two equations, see Fig. 1(c) and Ref. [3]:

$$\hat{v}_{p,S} = \hat{v}_{p,FS} + C \sum_{q=-\infty}^{\infty} \hat{Y}_{p-q,S}\hat{F}_{q,S}, \tag{7}$$

$$\hat{v}_{p,R} = C \sum_{q=-\infty}^{\infty} \hat{Y}_{p-q,R}\hat{F}_{q,R}. \tag{8}$$

After omission of the cross-order terms the complex power follows as [3]

$$Q_{\text{approx}} = \frac{1}{2} \sum_{p=-\infty}^{\infty} \frac{|\hat{v}_{p,FS}|^2 \hat{Y}_{p-p,R}}{|\hat{Y}_{p-p,S} + \hat{Y}_{p-p,R}|^2}. \tag{9}$$

The source descriptor is defined as the complex power that is required at the contact points of the free source without internal excitation in order to obtain the free source velocity [2]. Hence, the source descriptor equals half the product of the free source velocity and the complex conjugated blocked force [7],

$$S = \frac{1}{2}\int_0^C v_{\mathrm{FS}}(s) F^*_{\mathrm{BS}}(s)\,\mathrm{d}s = \frac{C}{2}\sum_{p=-\infty}^{\infty} \hat{v}_{p,\mathrm{FS}} \hat{F}^*_{p,\mathrm{BS}}. \tag{10}$$

The blocked force and the free source velocity are connected by the mobility of the source,

$$\hat{v}_{p,\mathrm{FS}} = C \sum_{q=-\infty}^{\infty} \hat{Y}_{p-q,S} \hat{F}_{q,\mathrm{BS}}. \tag{11}$$

When neglecting the cross-order terms in Eq. (11), the equal-order approximation of the source descriptor is obtained by means of substitution in Eq. (10),

$$S_{\mathrm{approx}} = \frac{1}{2}\sum_{p=-\infty}^{\infty} \frac{|\hat{v}_{p,\mathrm{FS}}|^2}{\hat{Y}^*_{p-p,S}} = \sum_{p=-\infty}^{\infty} S_{p,\mathrm{approx}}. \tag{12}$$

As indicated above, S_{approx} equals the superposition of all source descriptor orders [3].

The cross-order terms are composed of cross-order interface mobilities and force orders and contribute the components of a velocity order that are caused by different orders of force, see Eq. (5). In a set of previous publications [3–5], the influence of cross-order interface mobilities as well as the distribution of force orders have been investigated. The cross-order interface mobilities describe the spatial dependence of ordinary mobilities defined by the distance between excitation and response positions along the interface [3]. Conditions that provoke cross-order interface mobilities primarily are changes in the dynamic properties of the structure such as boundaries or structural discontinuities. The interface geometry can also provoke cross-order interface mobilities as is studied in Section 3. A similar effect can be observed for built-up structures with distinctively differing transfer paths, see Section 4.

The cross-order interface mobilities are of importance at intermediate Helmholtz numbers for plate-like structures [3] and at intermediate and large Helmholtz numbers for frame-like structures [4]. At small Helmholtz numbers, where the wavelength is substantially larger than the interface, the structure along the interface moves predominantly in-phase. In turn, the equal-order interface mobility of order zero dominates all other interface mobilities, see Refs. [3,4]. If the in-phase motion of the structure along the interface is suppressed, the cross-order interface mobilities can theoretically become significant. The effect of a possible suppression of the zero-order motion on the significance of the cross-order terms is investigated in Section 5.

The second part of the cross-order terms, i.e. the force orders, can be pivotal for the admissibility of neglecting the cross-order terms. If all force orders are equal, however, the significance of the cross-order interface mobilities applies for the significance of the cross-order terms. At frequencies where the source does not act as a rigid mass, the small magnitude range of the force orders suggests the latter to be a valid approximation, see Ref. [5]. If the source exhibits a mass-like behavior with coherent internal source mechanisms and the receiver shows a stiffness- or mass-like behavior, the contact forces will be either in phase or out of phase. With such a deterministic phase of the contact forces, a large range in magnitude is possible for the force orders and the significance of the cross-order terms can differ substantially from that of the cross-order interface mobilities [5]. In Section 6, therefore, the significance of the cross-order terms is studied for cases where the contact forces have such a deterministic phase.

3. Interface geometry

Conventionally, ordinary mobilities such as point and transfer mobilities are defined by the *location* of excitation and response positions. In conjunction with the influence of cross-order interface mobilities, however, a different definition appears sensible. In Refs. [3,4] it is suggested to define ordinary mobilities by the *distance* Δs between excitation and response positions s_0 and s along the interface, see Fig. 6. A transfer mobility defined in such a way has a fixed distance Δs

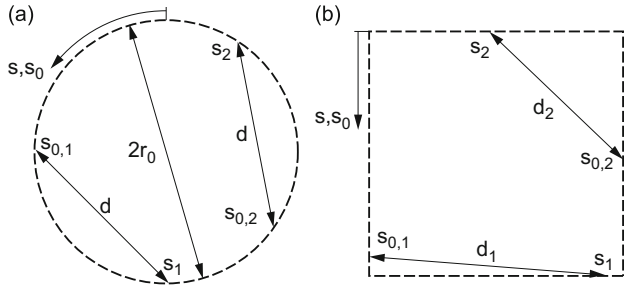

Fig. 6. Illustration of the influence of the interface geometry on the actual distance between excitation and response positions with $\Delta s = s_1 - s_{0,1} = s_2 - s_{0,2}$: (a) circular interface; (b) rectangular interface. – – – interface.

and is a function of the location along the interface. For a given interface, therefore, only one point mobility exists, which likewise is a function of the interface coordinate s. This definition originates from the fact that the cross-order interface mobilities are found to describe the dependence of ordinary mobilities on the location along the interface, see Refs. [3,4].

In the absence of structural discontinuities on a given plate at a given frequency, ordinary mobilities are dependent on the distance d between excitation and response positions only. For circular interface geometries on plate-like structures, this distance is given by $d = 2r_0 \sin(2\pi C/\Delta s)$, see Fig. 6. Under the condition that Δs is constant, d is independent of the location of excitation and response, see Fig. 6(a). When moving an ordinary mobility along the interface, therefore, the distance a wave has to travel from excitation to response position remains the same. Hence, in the absence of changes in the dynamic characteristics of the structure, ordinary mobilities defined by the distance Δs are independent of the location along a circular interface. It can therefore be concluded that a circular interface geometry does not strengthen cross-order interface mobilities.

For non-circular interface geometries on plate-like structures, the straight distance between excitation and response positions varies when moving the positions along the interface even if the distance Δs is retained, see Fig. 6(b). Consequently, the transfer mobilities change with the location along the interface and the cross-order interface mobilities are strengthened.

3.1. Rectangular interface with aspect ratio 3

For a rectangular interface with an aspect ratio of 3 on an infinite, homogeneous plate, see Fig. 7, the ordinary mobilities and interface mobilities for small, intermediate and large Helmholtz numbers are plotted in Fig. 8. The ordinary mobilities are calculated by means of Hankel functions, see Ref. [8], and the interface mobilities readily follow from Eq. (4). The upper graphs in Fig. 8 show the shape functions of the ordinary mobilities normalized by the point mobility of the infinite plate. In the bottom figures, the orders of magnitude of the lowest interface mobilities are plotted, also normalized by the infinite plate mobility. The interface mobilities which are crossed out are equal to zero due to symmetry, cf. Ref. [4]. In combination with the interface mobility shape functions from Figs. 4 and 5, the relationship between the ordinary mobilities and the interface mobilities becomes evident.

At small Helmholtz numbers, $k_B d \ll 1$, and in the absence of structural discontinuities, point and transfer mobilities are approximately equal, irrespective of the distance d between excitation and response positions along the interface. In Fig. 8(a), therefore, the ordinary mobility shape function is approximately constant. Hence, the cross-order interface mobilities are small compared with the predominant equal-order interface mobility of order zero, see Fig. 4(a). At intermediate and large Helmholtz numbers, the ordinary mobility shape functions show distinct variations along lines parallel to the main diagonal for which $s=s_0$. However, the cross-order interface mobilities are seen to be of lower order of magnitude than the dominating equal-order interface mobilities.

In order to study the significance of the cross-order terms after being superimposed, a uniform force-order distribution can be assumed, see Ref. [4]. If all force orders are equal, the complex power is proportional to the superposition of all interface mobilities, see Eq. (6). The sum of all interface mobilities equals the point mobility at the origin of the interface coordinates [4]. Furthermore, the superposition of all equal-order interface mobilities yields the mean point mobility along the interface [4]. In the absence of structural discontinuities, all point mobilities are equal, leading to a superposition of all cross-order interface mobilities equal to zero. Hence, the assumption of a uniform force-order distribution does not yield further information about the importance of the cross-order terms provoked by the interface geometry with regard to the complex power.

For the significance of the cross-order terms regarding the source descriptor and coupling function orders [4], however, the assumption of a uniform force-order distribution is more fruitful. By assuming a uniform distribution of the force-orders, the velocity orders in Eq. (5) become proportional to the superposition of series of interface mobilities. Such series

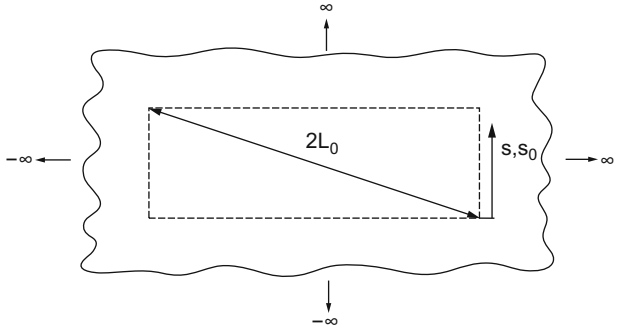

Fig. 7. Illustration of a rectangular interface with aspect ratio 3 on an infinite, homogeneous plate. – – – interface.

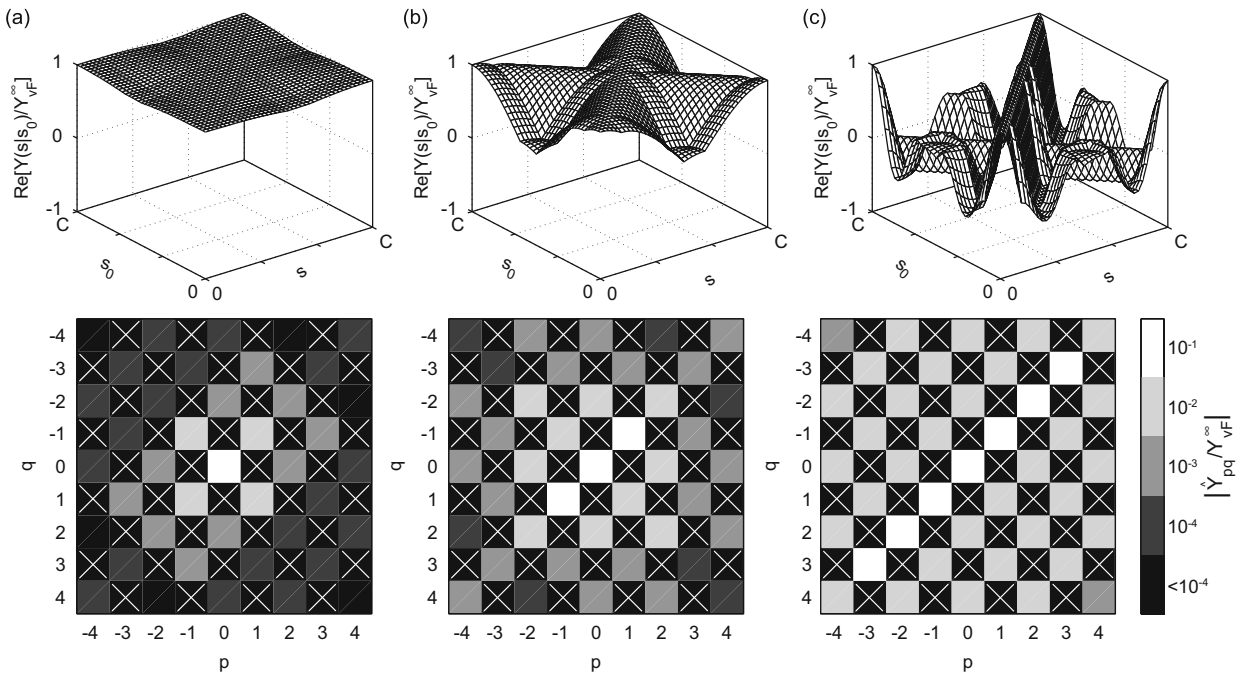

Fig. 8. Ordinary mobility shape functions in the upper figures with the corresponding interface mobilities in the lower figures for a rectangular interface with aspect ratio 3 on an infinite, homogeneous plate: (a) $k_B L_0$=0.25; (b) $k_B L_0$=1; (c) $k_B L_0$=4.

are found in the columns of the interface mobility matrices in Fig. 8. The superposition of cross-order interface mobilities is dependent on the location of the ideal point excitation which leads to a uniform force-order distribution [4]. For a different location of the ideal point excitation, therefore, the velocity orders can change. Hence, the interval between the maximum and minimum magnitude values of the velocity orders are used to cover all cases.

In Fig. 9 are plotted three velocity orders for the rectangular interface with an aspect ratio of 3 on an infinite, homogeneous plate. The gray-shaded areas represent the magnitude intervals of the velocity orders that is formed for the different locations of the ideal point excitation leading to a uniform force-order distribution. The solid line depicts the approximation by the equal-order interface mobility which is independent of the location of the ideal point excitation [4]. At small and intermediate Helmholtz numbers, a particularly close agreement is observed between the zero-order velocity and equal-order interface mobility. The cross-order interface mobilities are found to be influential at large Helmholtz numbers for the zero-order velocity and at all frequencies for higher-order velocities.

When comparing a circular and a non-circular interface on an infinite, homogeneous plate, it becomes evident that only transfer mobilities are affected by the interface geometry. Along a circular interface geometry, a transfer mobility defined by Δs is independent of the location along the interface. This is due to the fact that the distance d between excitation and response positions remains constant, see Fig. 6. For a non-circular interface geometry, the distance d changes for different locations of the transfer mobility along the interface. If the straight distance between excitation and response positions changes, the transfer mobility changes as well. For point mobilities, the distance d equals zero irrespective of both the location of excitation and response along the interface and the interface geometry. It is therefore argued that the interface geometry does not affect point mobilities. Additionally, the transfer mobilities vanish asymptotically at high frequencies by virtue of divergence. Furthermore, the cross-order interface mobilities provoked by a non-circular interface geometry are found to be of smaller order of magnitude than those provoked by structural discontinuities, cf. Ref. [3]. In comparison with the importance of structural discontinuities, therefore, the interface geometry can be argued to be of subordinate significance with regard to a strengthening of cross-order interface mobilities. An analysis of the importance of the cross-order terms for a complete installation with a rectangular interface of aspect ratio 3 is discussed in Section 7.1.

4. Structures with distinctively differing transfer paths

As discussed in the previous section, non-circular interface geometries on plate-like structures will strengthen cross-order interface mobilities due the fact that the transfer mobilities vary with the location along the interface. A similar effect can be observed for built-up structures where the transfer path between adjacent contact points differs substantially along the interface. An example of such a source structure is presented in Fig. 10. The transfer of vibrations between points s_2 and s_3 of the source follows the shortest possible path. As furthermore indicated by the arrows, the waves have to travel a

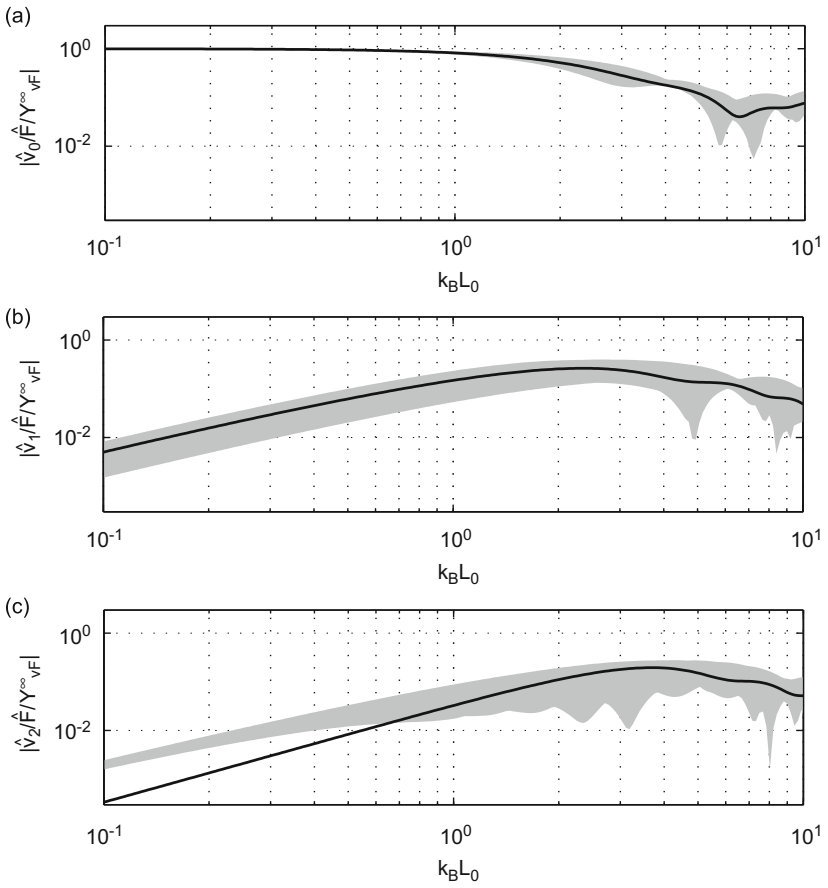

Fig. 9. Superposition of interface mobilities for a few velocity orders along a rectangular interface with aspect ratio 3 on an infinite, homogeneous plate, where the gray-shaded areas represent the magnitude intervals of the velocity orders: (a) $\hat{v}_0$; (b) $\hat{v}_1$; (c) $\hat{v}_2$. —, equal-order interface mobility.

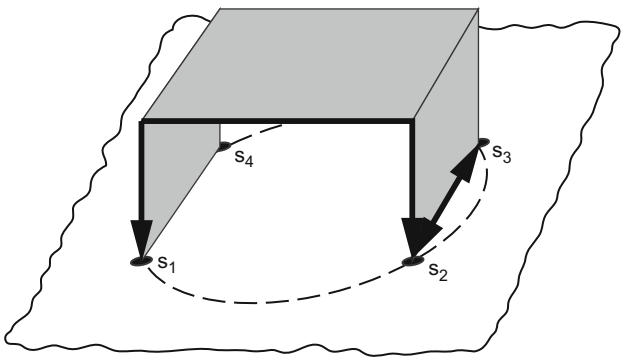

Fig. 10. Illustration of a hypothetical source structure with distinctively differing transfer paths. – – – interface; • contact point.

detour between the contact points s_1 and s_2 along the source structure. Hence, the transfer path from the front to the rear of the source structure presented in Fig. 10 is substantially shorter than that from one side to the other. At high frequencies, therefore, the transfer mobilities between two adjacent contact points will vary for different locations along the interface. Owing to this variation of the transfer mobilities, the cross-order interface mobilities are strengthened.

4.1. Receiver structure consisting of two parallel infinite beams

In the following, the effect of distinctively differing transfer paths on the importance of the cross-order interface mobilities is studied on the theoretically extreme case of the receiver structure shown in Fig. 11. This structure consists of

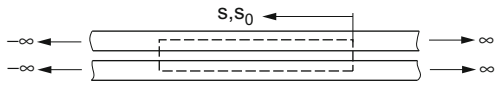

Fig. 11. Illustration of a rectangular interface on a receiver structure consisting of two beams that are not connected. – – – interface.

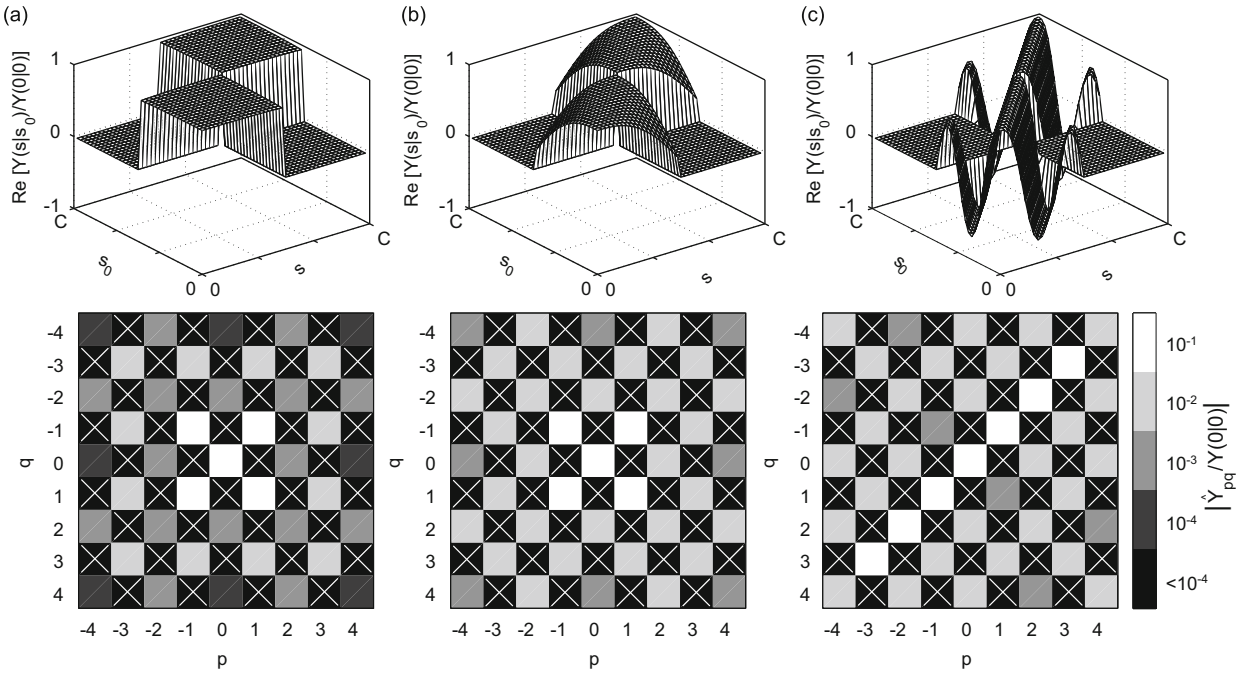

Fig. 12. Ordinary mobility shape functions in the upper figures with the corresponding interface mobilities in the lower figures for a rectangular interface on two parallel, infinite, homogeneous beams: (a) $k_B L_0 = 0.25$; (b) $k_B L_0 = 1$; (c) $k_B L_0 = 4$.

two parallel infinite beams that are not connected. In a source–receiver installation, the two beams will be interfaced with the source structure. On such a receiver structure, the mobilities describing the transfer of vibrations from one beam to the other are equal to zero.

In Fig. 12 are plotted the ordinary mobility shape functions and the corresponding interface mobilities for a rectangular interface on two parallel, infinite, homogeneous beams at small, intermediate and large Helmholtz numbers. The ordinary mobilities are calculated by the wave approach employing Euler–Bernoulli theory, see Ref. [8], and the interface mobilities follow from Eq. (4). The interface is sampled in a way, that the 24 sampling points are located on the beams.

The ordinary mobility shape functions show distinct variations along lines parallel to the main diagonal for which s equals s_0 at all frequencies. Due to the symmetry of the interface system under consideration, $\hat{Y}_{11}$ and $\hat{Y}_{-1-1}$ are of the same order of magnitude as the dominating equal-order interface mobilities at small and intermediate Helmholtz numbers. At high frequencies, the individual cross-order interface mobilities are found to be of lower order of magnitude than the dominating equal-order interface mobilities.

In the theoretical case discussed above, the transfer mobilities vary substantially at all frequencies, see Fig. 12. For practical cases, the transfer mobilities are likely to vary within a certain frequency band only, depending on the mechanisms or structural conditions resulting in the variation. The transfer mobilities will vary for different locations along the interface if the damping or attenuation varies between different transfer paths. Damping in terms of conversion of mechanical energy into heat as well as attenuation due to e.g. blocking masses or elastic interlayer are frequency dependent mechanisms [8]. The amount of damping referring to a conversion of mechanical energy into heat, for instance, depends on the number of oscillations it takes a wave to get from excitation to response position. At small Helmholtz numbers, therefore, the difference in damping between the two transfer paths highlighted in Fig. 10 will be negligible. At large Helmholtz numbers, the amount of damping will differ between the two transfer paths, yielding stronger cross-order interface mobilities than at small Helmholtz numbers.

For the interface system under consideration, see Fig. 11, all point mobilities are equal along the interface. As discussed in the previous section, therefore, assuming a uniform force-order distribution does not yield further information about the importance of the cross-order terms with regard to the complex power. For the source descriptor and coupling function orders, in Fig. 13, a few velocity orders are compared with the equal-order approximation. In Fig. 13(a), an extremely close

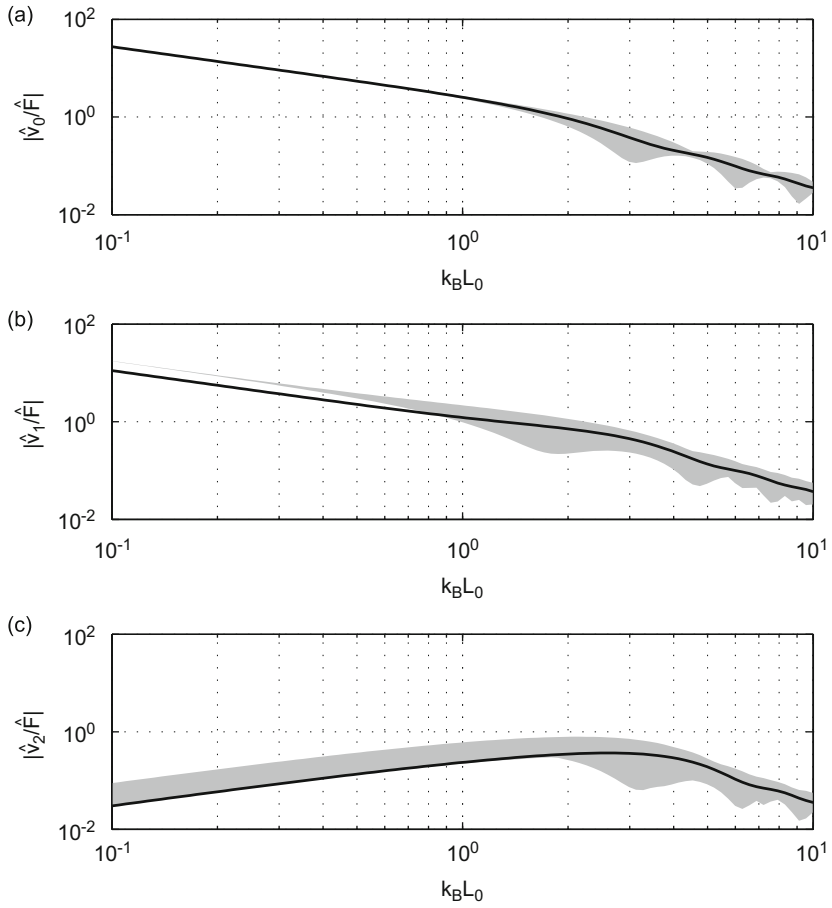

Fig. 13. Superposition of interface mobilities for a few velocity orders along a rectangular interface on two parallel, infinite, homogeneous beams, where the gray-shaded areas represent the magnitude intervals of the velocity orders: (a) $\hat{v}_0$; (b) $\hat{v}_1$; (c) $\hat{v}_2$. —, equal-order interface mobility.

agreement is observed between the zero-order velocity and the equal-order approximation at small and intermediate Helmholtz numbers. At large Helmholtz numbers for the zero-order velocity and at all frequencies for higher-order velocities, the cross-order interface mobilities are found to be present but of subordinate influence.

Although it is evident from Fig. 12 that certain cross-order interface mobilities are of the same order of magnitude as the dominating equal-order interface mobilities, it can be presumed from Fig. 13 that their contribution after superposition is negligible.

5. Suppression of zero-order motion

The cross-order interface mobilities have been found to be insignificant at small Helmholtz numbers due to the predominance of the equal-order interface mobility of order zero [3,4]. However, if the zero-order motion of the structure along the interface is suppressed, $\hat{Y}_{00}$ can become small compared with other interface mobilities.

5.1. Simply supported infinite plate

Consider the case where a circular interface is located centered on the simple support of an infinite, homogeneous plate as illustrated in Fig. 14(a). The point and transfer mobilities are calculated by the mirror image approach [9]. When subject to point excitation at small Helmholtz numbers, the structure along the interface will mainly respond by rotation around the support axis. Although some small high-order content is present, the first-order response will be dominant and the zero-order motion will be fully suppressed. As shown in Fig. 15, therefore, the zero-order equal-order interface mobility is equal to zero. For a given order number p, furthermore, the cross-order interface mobilities of type $\hat{Y}_{pp}$ are of the same order of magnitude as the equal-order interface mobilities $\hat{Y}_{p-p}$.

Upon exciting the simply supported plate with a single point force directly on the support, the velocity along the interface and consequently the complex power will be equal to zero. In contrast, a point-force excitation at a location other

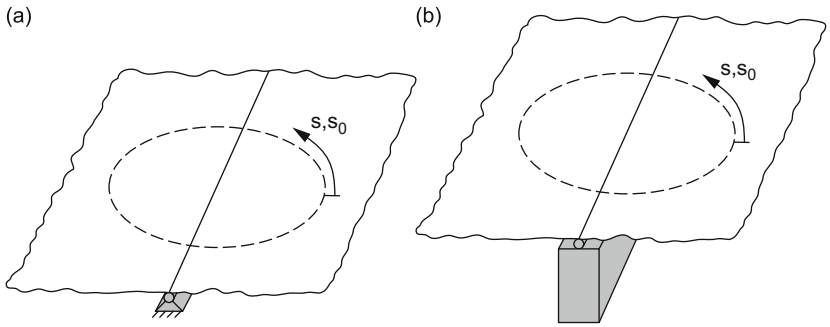

Fig. 14. Schematic illustration of two infinite plates on a simple support and a beam stiffener with circular interfaces: (a) interface on the simple support of an infinite plate; (b) interface on an infinite, beam-stiffened plate. – – – interface.

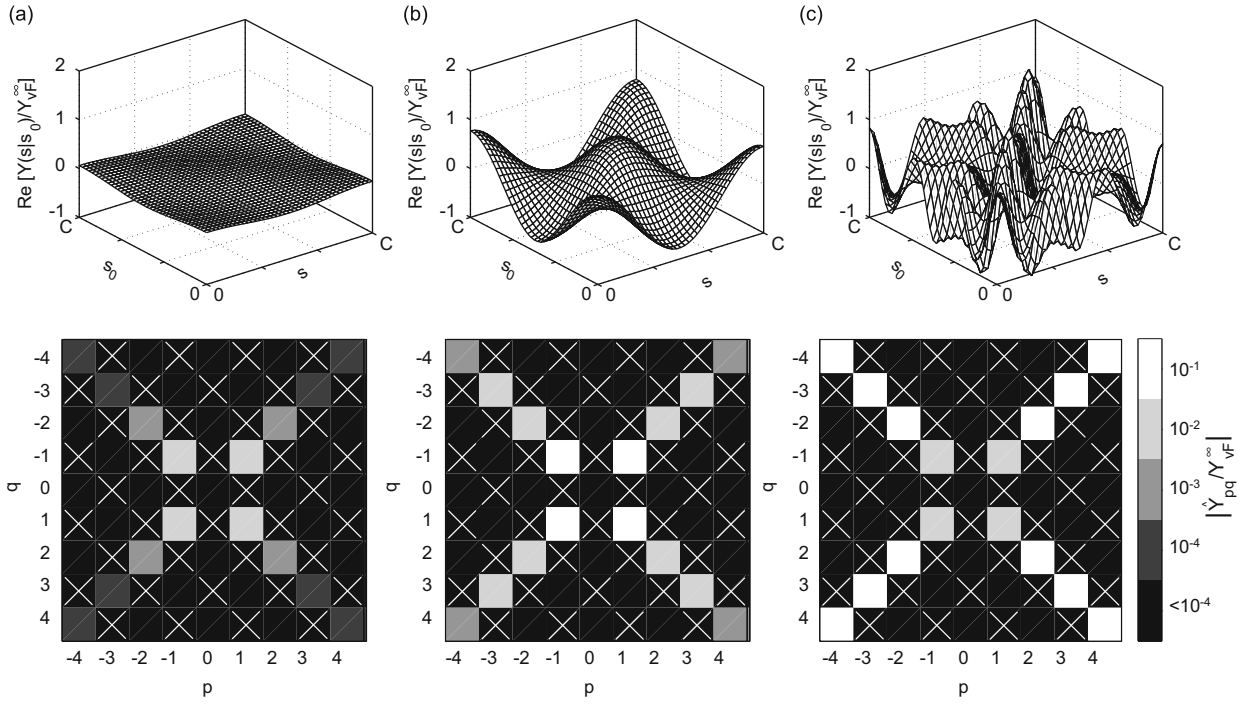

Fig. 15. Ordinary mobility shape functions in the upper figures with the corresponding interface mobilities in the lower figures for a circular interface on the simple support of an infinite plate: (a) $k_B r_0$=0.25; (b) $k_B r_0$=1; (c) $k_B r_0$=4.

than directly on the support will yield non-zero velocity and complex power. These two cases demonstrate the wide range of possible results of the power and velocity orders under the assumption of a uniform force-order distribution, where all force orders are equal [4]. The equal-order interface mobilities and thereby the equal-order approximations of the complex power and the velocity orders are constant for all possible locations of the origin of the interface coordinates, see Ref. [4]. The results that can be obtained by assuming a uniform force-order distribution, therefore, are of minor use. Whether the cross-order terms are negligible or not depends on the force orders, as discussed in Sections 6 and 7.2. However, the theoretical case of a simple support with a driving point mobility of zero is judged to be unrealistic with respect to engineering practice. A similar construction that can be found in practice is a thin plate connected to a beam stiffener as illustrated in Fig. 14(b).

5.2. Beam-stiffened infinite plate

The ordinary mobility shape functions with the corresponding interface mobilities for the case of a 20 mm thick chipboard plate supported by a concrete beam with 100 mm width and 200 mm height are plotted in Fig. 16. The ordinary mobilities of the plate are calculated by using Hankel functions, those of the beam stiffener are obtained by the wave approach employing Euler–Bernoulli theory [8]. The combined structure is realized by means of substitution forces,

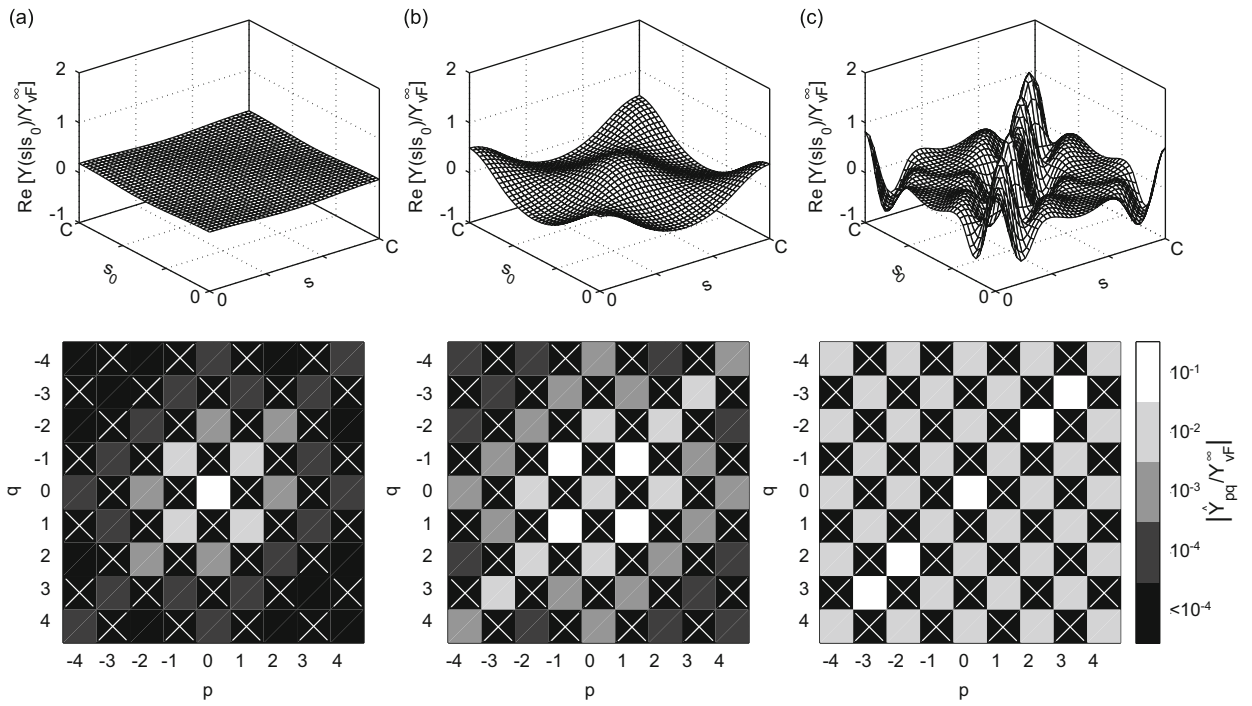

Fig. 16. Ordinary mobility shape functions in the upper figures with the corresponding interface mobilities in the lower figures for a circular interface on an infinite, beam-stiffened plate: (a) $k_B r_0$=0.25; (b) $k_B r_0$=1; (c) $k_B r_0$=4.

see Ref. [10], where the plate is simply supported on the beam, see Fig. 14(b). Due to the non-zero mobility of the beam stiffener, in Fig. 16(a), the zero-order motion is clearly identifiable although suppressed when compared with Fig. 8(a). In turn, the equal-order interface mobility of order zero retains the predominance over all other interface mobilities at small Helmholtz numbers.

Owing to the non-zero mobility along the stiffener of the plate, the assumption of a uniform force-order distribution does yield further information about the influence of the cross-order interface mobilities after being superimposed. In Fig. 17 is plotted the magnitude of a few velocity orders along the circular interface of the beam-stiffened plate under consideration in comparison with the equal-order approximations. The quality of the equal-order approximation with regard to the superposition of all orders is presented in Fig. 18.

At small Helmholtz numbers, the velocities of orders different from zero are found to be insignificant due to the predominance of the zero-order velocity. In this frequency range, a high degree of similarity is observed between the equal-order approximation and the zero-order velocity as well as the superposition of all orders. If the wavelength is substantially larger than the interface, the mobility along the interface is governed by the stiffener. The ordinary mobility shape function therefore is approximately equal for all positions along the interface, see Fig. 16(a). Although the zero-order motion is suppressed in comparison with the unstiffened plate, the persistent predominance of $\hat{Y}_{00}$ results in a negligible contribution of the cross-order interface mobilities at low frequencies. It can therefore be presumed that a significant suppression of the zero-order motion at small Helmholtz numbers is rather unlikely in practice.

6. Deterministic phase of contact forces

If the source is mass controlled with coherent internal source mechanisms and the receiver stiffness or mass controlled, the contact forces will be either in phase or out of phase [11,12]. With such a deterministic phase of the contact forces at low frequencies, a large range in magnitude is possible for the force orders [5]. In the present section, results from Monte Carlo simulations are presented and discussed regarding the importance of a deterministic phase of the forces at the contact points for the significance of the cross-order terms. A cuboidal source structure is modeled as a rigid mass connected to various receiver structures.

The point and transfer mobilities of the source structure are derived from the equations of motion of a rigid body, assuming small translations and rotations [13]. An excitation force at (x_0,y_0,z_0) can be subdivided into moments due to the leverages x_0, y_0 and z_0, respectively, and a force acting at the center of mass, where $x=y=z=0$. The coupling between an excitation force in the z-direction at (x_0,y_0) and the translational velocity response in the z-direction at (x,y) therefore

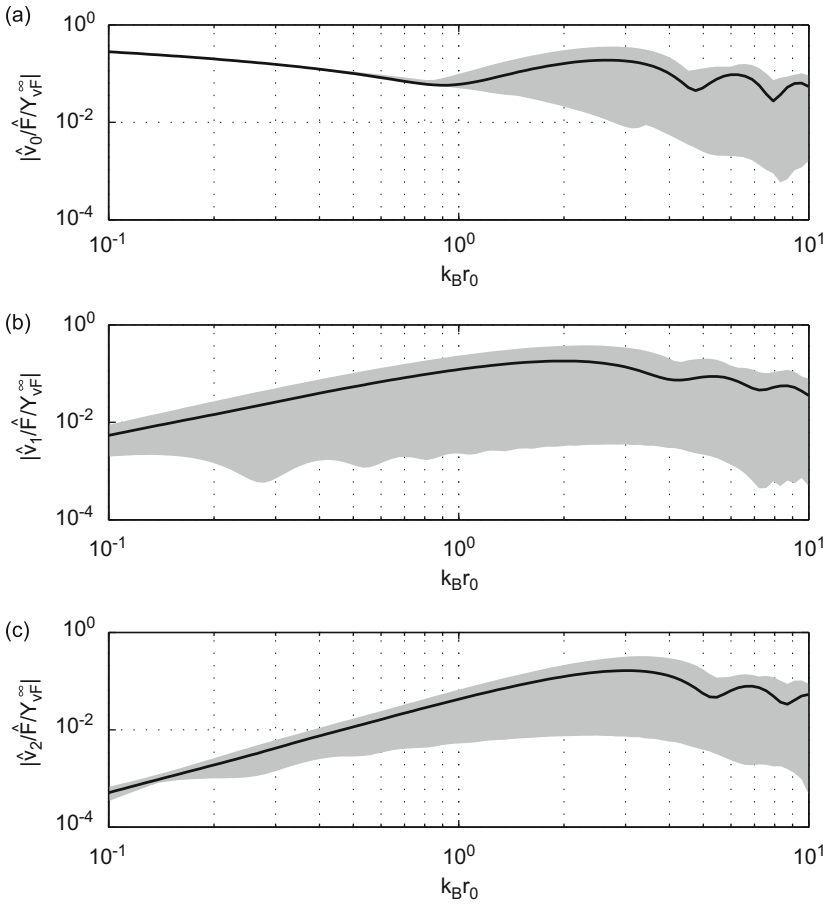

Fig. 17. Superposition of interface mobilities relating to the velocity orders for a circular interface on an infinite, beam-stiffened plate, where the gray-shaded areas represent the magnitude intervals of the velocity orders: (a) $\hat{v}_0$; (b) $\hat{v}_1$; (c) $\hat{v}_2$. —, equal-order interface mobility.

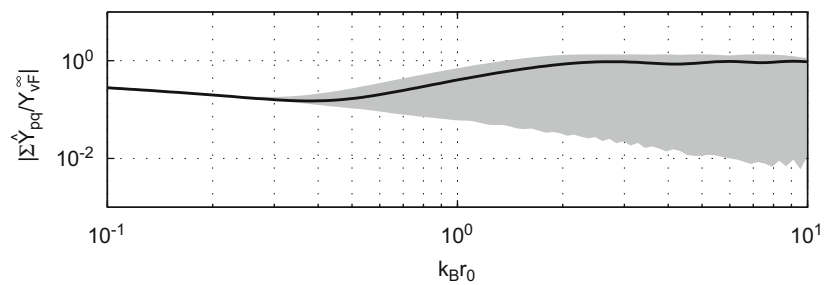

Fig. 18. Superposition of interface mobilities relating to the complex power for a circular interface on an infinite, beam-stiffened plate, where the gray-shaded area represents the magnitude interval of the superposition of interface mobilities. —, equal-order approximation.

consists of three parts,

$$Y(x,y|x_0,y_0)=\frac{1}{j\omega}\left(\frac{1}{m}+\frac{xx_0}{I_{yy}}+\frac{yy_0}{I_{xx}}\right). \tag{13}$$

The internal source mechanisms are either represented by a single force or a pure moment excitation. In order to avoid the truncation of the series expansion to affect the results, the source and receiver structures are connected at 24 equi-distant contact points. Except for the frame-like structure, a circular interface of radius r_0 is used. The length, width and height of the source ranges from $2r_0$ to $4r_0$. The parameters which are varied in the Monte Carlo simulations are the dimensions of the source structure, the location and orientation of the interface on the source as well as the location of the internal source excitation.

With Eq. (13), both the free source velocity and the source mobility can be calculated. The forces at the point contact points are calculated by means of the matrix formulation [8],

$$\mathbf{F}_R = (\mathbf{Y}_S + \mathbf{Y}_R)^{-1}\mathbf{v}_{FS}, \tag{14}$$

and the exact transmitted power follows by

$$W = \tfrac{1}{2}\mathrm{Re}[\mathbf{F}_R^{\mathrm{T}}\mathbf{Y}_R^{\mathrm{T}}\mathbf{F}_R^{*}]. \tag{15}$$

In the numerical simulations, the matrix formulation is considered to yield the exact values and is therefore used as reference for the equal-order approximations.

In the following, the importance of the cross-order terms is indicated by the median and maximum transmitted-power ratios. Such ratios describe the factor between the equal-order approximation of the interface mobility approach and the complete description from the matrix formulation. In order to obtain ratios not smaller than one, the larger value as indicated by the subscript U is divided by the smaller value which is indicated by the subscript L, e.g. W_U/W_L. As exceedingly large ratios can occur, the median ratio is argued to be a more meaningful indicator for the average than the mean ratio. The median ratios are indicated by an over-bar, e.g. $\overline{W_U/W_L}$. The ratios smaller than 10 are rounded to the first decimal place and ratios between 10 and 100 are rounded to the nearest integer. For ratios larger than 100, merely the order of magnitude is presented.

As described in Section 2, two equal-order approximations of the transmitted power have to be distinguished when neglecting the cross-order terms, i.e. one based on the contact forces from Eq. (6) and another based on the free source velocity in Eq. (9). In addition to these two quantities, the relation between the zero- and first-order forces is studied in the following simulations. This can be of importance for cases where a weak zero-order force neutralizes the predominance of the equal-order interface mobility of order zero. The comparison of the force orders is confined to zero- and first-order forces due to the fact that a rigid body only exhibits rotational and translational vibrations and that higher interface mobility orders tend to be insignificant at low frequencies, see Refs. [3,4].

6.1. Plate-like receiver structure

In a first set of simulations of source–receiver installations, a simply supported finite, homogeneous plate with asymmetric location of the interface is used as receiving structure, see Fig. 19. The ordinary mobilities are obtained by means of a modal summation, see Ref. [14]. In Table 1, the results for internal force and moment excitation of the source are presented, where 100,000 different installations are simulated for each case. By changing the density of the source structure, matched and unmatched source and receiver mobilities are realized.

The first two columns in Table 1 include the median and maximum ratios of the respective quantities. The third column in Table 1(a) shows the percentage of cases where the zero-order force dominates $\hat{F}_1$ and $\hat{F}_{-1}$. In Table 1(b), the third column indicates the percentage of cases where the equal-order approximation yields an overestimate of the exact data. The values in brackets represent the results for the equal-order approximation based on the contact forces, see Eq. (6), and the values without brackets represent the results based on the free source velocity, see Eq. (9).

As shown in Table 1(a), exceedingly large force-order ratios are possible for the case of a deterministic phase of the contact forces. If the internal source mechanisms of the source result in a single force excitation, on average the zero- and first-order forces are of the same order of magnitude. Here, the force of order zero tends to be smaller than the first-order forces. An internal moment excitation is found to always result in spatial force distributions with dominating first-order components in comparison with the zero-order component.

For the finite plate receiver, a particularly close agreement is observed between the exact transmitted power and the approximations by the interface mobility approach, see Table 1(b). Although the force of order zero is smaller than the first-order forces for an internal moment excitation, the transmitted-power ratios are similar to those of an internal force excitation. On average, both equal-order approximations show a similar agreement with the exact transmitted power.

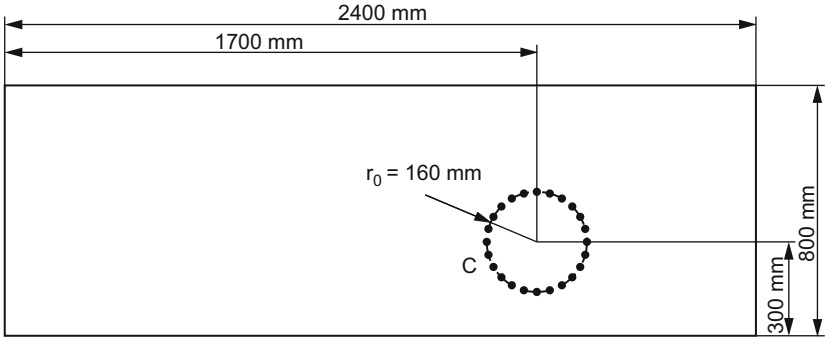

Fig. 19. Simply supported, finite plate with circular interface. – – – interface; • discretization point.

Table 1
Rigid source structure installed on a simply supported finite plate, see Fig. 19, at $k_B r_0$=0.5, where the values in brackets represent the results based on the contact forces and those without brackets the results based on the free source velocity: (a) force orders; (b) transmitted power.

(a) Force orders	$\overline{\lvert\hat{F}_{0,\pm1}\rvert_U/\lvert\hat{F}_{0,\pm1}\rvert_L}$	$\max(\lvert\hat{F}_{0,\pm1}\rvert_U/\lvert\hat{F}_{0,\pm1}\rvert_L)$	$\lvert\hat{F}_0\rvert \geq \lvert\hat{F}_{\pm1}\rvert$ (%)
Internal $Y_R < Y_S$	1.4	10^2	39
Force $Y_R = Y_S$	2.2	10^3	9
Excitation $Y_R > Y_S$	2.6	10^2	3
Internal $Y_R < Y_S$	10^2	10^5	0
Moment $Y_R = Y_S$	7.3	10^3	0
Excitation $Y_R > Y_S$	4.6	10^4	0
(b) Transmitted power	$\overline{W_U/W_L}$	$\max(W_U/W_L)$	$W_{approx} > W$ (%)
Internal $Y_R < Y_S$	1.5 (1.3)	15 (3.8)	58 (74)
Force $Y_R = Y_S$	1.2 (1.4)	6.1 (3.8)	70 (77)
Excitation $Y_R > Y_S$	1.3 (2.1)	2.0 (3.8)	44 (85)
Internal $Y_R < Y_S$	1.2 (1.1)	2.6 (1.2)	81 (80)
Moment $Y_R = Y_S$	1.3 (1.4)	4.4 (3.4)	94 (99)
Excitation $Y_R > Y_S$	1.1 (2.2)	1.9 (3.7)	35 (100)

The relation between the source and receiver mobilities is not found to have a systematic influence on ratios of the force orders or of the transmitted power.

6.2. Frame-like receiver structure

In a next set of simulations a frame-like structure consisting of four infinite, homogeneous beams as shown in Fig. 20 is used as the receiver. The ordinary mobilities along the rectangular interface of diagonal $2L_0$ are obtained by treating the receiver as a built-up structure. Substitution forces and moments are included for both bending and torsional waves [10]. The point and transfer mobilities of the four infinite beams are calculated by the wave approach employing Euler–Bernoulli theory [8].

For an internal force excitation, the distribution of the force orders is highly dependent on the relationship between the source and receiver mobilities, see Table 2(a). With decreasing source mobility, the zero-order force vanishes in comparison with the first-order forces. If the internal source mechanisms result in a single moment excitation of the source, the force of order zero is found to be substantially smaller than the first-order forces in 100 percent of the simulated cases.

With maximum ratios smaller than two, the equal-order approximation based on the contact forces gives an almost exact prediction of the transmitted power, see Table 2(b). In contrast, larger transmitted-power ratios are found for the estimate of the interface mobilities based on the free source velocity. This appears reasonable, since the cross-order terms have to be neglected more often in the latter case compared with the equal-order approximation based on the contact forces, see Section 2. Although the zero-order force is substantially smaller than $\hat{F}_1$ and $\hat{F}_{-1}$ for an internal moment excitation of the source, the equal-order approximations yield useful estimates. It can be surmised that in such cases, the equal-order term $\hat{Y}_{00,R}\hat{F}_{0,R}$ is insignificant, although $\hat{Y}_{00,R}$ is substantially larger than all other receiver interface mobilities at small Helmholtz numbers. It is interesting to note that an internal moment excitation of the source yields an underestimation of the transmitted power by the equal-order approximation based on the contact forces and an overestimation by the relaxed formulation based on the free source velocity.

6.3. Receiver structures with suppressed zero-order motion

In the following, results from Monte Carlo simulations are presented for installations with the two receiver structures studied in Section 5 in conjunction with a possible suppression of the zero-order motion at small Helmholtz numbers. Since source structures will most likely feature a mass-like behavior at low frequencies, simulations of rigid structures installed on the two receiver structures analyzed in Section 5 are meaningful. Although the phase of the contact forces does not necessarily have to be deterministic for such cases, the results give valuable information about the significance of the cross-order terms.

In Table 3, the results from the Monte Carlo simulations are presented for a circular interface located centered on the simple support of an infinite, plate-like receiving structure as shown in Fig. 14(a). Since the point mobilities of the receiver structure are equal to zero along the simple support, the mean receiver point mobility is used as reference when determining the density of the rigid source structure for the case $Y_R > Y_S$.

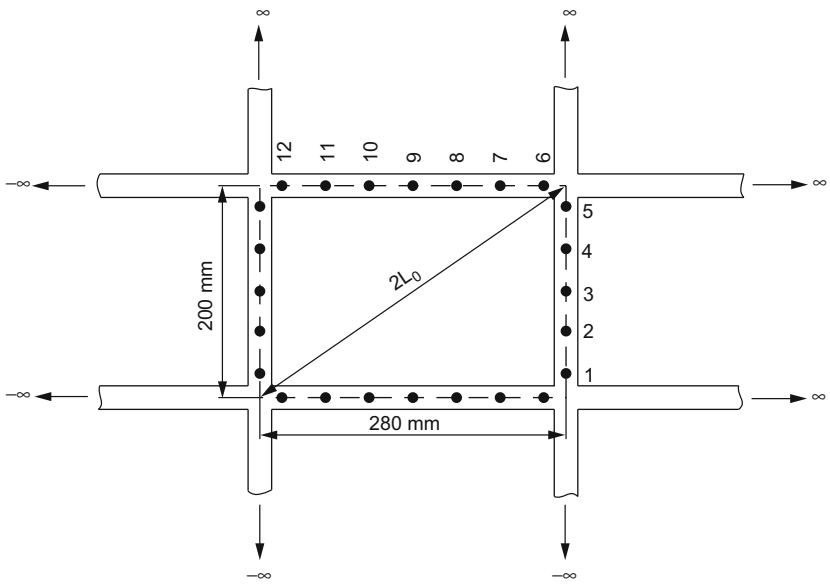

Fig. 20. Rectangular frame-like structure consisting of infinite, homogeneous beams with an interface sampled at M=24 points. – – – interface; • discretization point.

Table 2
Rigid source structure installed on a frame-like receiver structure consisting of four infinite beams, see Fig. 20, at $k_B L_0$=0.1, where the values in brackets represent the results based on the contact forces and those without brackets the results based on the free source velocity: (a) force orders; (b) transmitted power.

(a) Force orders	$\overline{\lvert\hat{F}_{0,\pm1}\rvert_U/\lvert\hat{F}_{0,\pm1}\rvert_L}$	$\max(\lvert\hat{F}_{0,\pm1}\rvert_U/\lvert\hat{F}_{0,\pm1}\rvert_L)$	$\lvert\hat{F}_0\rvert \geq \lvert\hat{F}_{\pm1}\rvert$ (%)
Internal $Y_R < Y_S$	1.5	10^2	35
Force Y_R=Y_S	3.3	10^2	5
Excitation $Y_R > Y_S$	10^2	10^4	0
Internal $Y_R < Y_S$	10^3	10^7	0
Moment Y_R=Y_S	10^2	10^6	0
Excitation $Y_R > Y_S$	10^2	10^6	0
(b) Transmitted power	$\overline{W_U/W_L}$	$\max(W_U/W_L)$	$W_{approx} > W$ (%)
Internal $Y_R < Y_S$	1.3 (1.0)	7.8 (1.1)	56 (99)
Force Y_R=Y_S	1.9 (1.0)	8.0 (1.6)	94 (45)
Excitation $Y_R > Y_S$	2.8 (1.4)	93 (1.7)	96 (0)
Internal $Y_R < Y_S$	6.9 (1.5)	15 (1.7)	100 (0)
Moment Y_R=Y_S	6.9 (1.5)	13 (1.7)	100 (0)
Excitation $Y_R > Y_S$	2.9 (1.5)	82 (1.7)	96 (0)

The distributions of the zero- and first-order forces show similar characteristics as for the case of the simply supported finite plate receiver, see Section 6.1. In an overall sense, the results are found to be equal for an internal force excitation and an internal moment excitation of the source.

If the data available are the free source velocity, the median ratios do not exceed values of approximately 8 for the transmitted power. On average, the equal-order approximation based on the contact forces, however, differs from the exact values by four orders of magnitude. Here, the cross-order power terms $\hat{F}_{q,R}\hat{Y}_{qq,R}\hat{F}_{-q,R}$ are approximately equal to the equal-order power terms $\hat{Y}_{q-q,R}|\hat{F}_{q,R}|^2$, but of opposing sign. All other receiver cross-order interface mobilities as well as $\hat{Y}_{00,R}$ are equal to zero, see Fig. 15. Hence, a power circulation occurs between the equal-order and cross-order power terms, resulting in large misinterpretations of the equal-order approximation based on the contact forces.

In the derivation of the equal-order approximations based on the free source velocity, the source cross-order terms $\hat{Y}_{p-q,S}\hat{F}_{q,S}$ are omitted in addition to the receiver cross-order terms, see Section 2. In spite of this fact, the equal-order approximation based on the free source velocity yields better estimates than that based on the contact forces. Moreover, the cross-order terms are found to be of subordinate significance if the data available are the free source velocity.

Table 3
Rigid source structure installed on the simple support of an infinite plate, see Fig. 14(a), at $k_B r_0$=0.1, where the values in brackets represent the results based on the contact forces and those without brackets the results based on the free source velocity: (a) force orders; (b) transmitted power.

(a) Force orders	$\overline{\lvert\hat{F}_{0,\pm1}\rvert_U/\lvert\hat{F}_{0,\pm1}\rvert_L}$	$\max(\lvert\hat{F}_{0,\pm1}\rvert_U/\lvert\hat{F}_{0,\pm1}\rvert_L)$	$\lvert\hat{F}_0\rvert \geq \lvert\hat{F}_{\pm1}\rvert$ (%)
Internal $Y_R < Y_S$	1.5	10^2	34
Force $Y_R = Y_S$	1.8	10^2	58
Excitation $Y_R > Y_S$	1.7	10^3	66
Internal $Y_R < Y_S$	10^2	10^6	0
Moment $Y_R = Y_S$	8.8	10^6	5
Excitation $Y_R > Y_S$	9.3	10^7	9
(b) Transmitted power	$\overline{W_U/W_L}$	$\max(W_U/W_L)$	$W_{approx} > W$ (%)
Internal $Y_R < Y_S$	2.4 (10^4)	10^9 (10^9)	49 (100)
Force $Y_R = Y_S$	7.8 (10^4)	10^{10} ((10^{10})	98 (100)
Excitation $Y_R > Y_S$	4.7 (10^4)	10^8 (10^{12})	97 (100)
Internal $Y_R < Y_S$	2.1 (10^4)	10^8 (10^8)	46 (100)
Moment $Y_R = Y_S$	7.6 (10^4)	10^{10} (10^{11})	100 (100)
Excitation $Y_R > Y_S$	4.4 (10^4)	10^9 (10^{13})	100 (100)

Table 4
Rigid source structure installed on a beam-stiffened infinite plate, see Fig. 14(b), at $k_B r_0$=0.1, where the values in brackets represent the results based on the contact forces and those without brackets the results based on the free source velocity: (a) force orders; (b) transmitted power.

(a) Force orders	$\overline{\lvert\hat{F}_{0,\pm1}\rvert_U/\lvert\hat{F}_{0,\pm1}\rvert_L}$	$\max(\lvert\hat{F}_{0,\pm1}\rvert_U/\lvert\hat{F}_{0,\pm1}\rvert_L)$	$\lvert\hat{F}_0\rvert \geq \lvert\hat{F}_{\pm1}\rvert$ (%)
Internal $Y_R < Y_S$	1.5	10^2	35
Force $Y_R = Y_S$	3.8	10^3	4
Excitation $Y_R > Y_S$	64	10^4	0
Internal $Y_R < Y_S$	10^3	10^7	0
Moment $Y_R = Y_S$	10^2	10^6	0
Excitation $Y_R > Y_S$	10^2	10^6	0
(b) Transmitted power	$\overline{W_U/W_L}$	$\max(W_U/W_L)$	$W_{approx} > W$ (%)
Internal $Y_R < Y_S$	1.3 (1.0)	88 (1.1)	37 (53)
Force $Y_R = Y_S$	1.3 (1.1)	10^2 (2.7)	44 (42)
Excitation $Y_R > Y_S$	1.4 (6.1)	10^3 (10)	51 (91)
Internal $Y_R < Y_S$	3.3 (1.8)	10^2 (10)	84 (50)
Moment $Y_R = Y_S$	2.0 (1.7)	10^2 (10)	52 (42)
Excitation $Y_R > Y_S$	1.5 (7.7)	10^3 (10)	50 (91)

For the more realistic receiver structure of a beam-stiffened plate as studied in Section 5, the results from the Monte Carlo simulations are plotted in Table 4. The zero-order force is found to be of the same order of magnitude as the first-order forces only for an internal force excitation and if the receiver mobilities are smaller or of the same order than the source mobilities. For the other cases, the first-order forces are always substantially larger than the zero-order force.

In contrast to the preceding case of a simple support as presented in Table 3, the median ratios shown in Table 4 indicate a close agreement between the equal-order approximation based on the contact forces and the complete calculation. The predominance of the first-order forces for an internal moment excitation of the source is found to result in slightly stronger cross-order terms. However, the small median ratios shown in Table 4 indicate a subordinate significance of the cross-order terms for all cases.

As shown in Table 3, it is possible to construct theoretical source–receiver installations for which the equal-order approximation based on the contact forces fails to give a useful estimate of the transmitted power and the vibration amplitude at small Helmholtz numbers. However, translating such theoretical cases into practice results in installations for which the equal-order approximations manage to resemble the transmitted power.

7. Experimental comparisons

In this section are investigated experimentally the four conditions presented in Sections 3–6. Two source–receiver installations are selected, suitably designed to allow for a possible strengthening of the cross-order terms according to such

four conditions. The installations have four contact points where the Nyquist criterion allows the calculation of three orders only, i.e. -1, 0 and 1.

For the measurements of the free source velocities and the source mobilities, the source structures are suspended with elastic straps in order to allow them to vibrate freely. It is assured that the eigenfrequency of the mass–spring system formed by the freely suspended source is located at a frequency below the frequency range of interest. The velocity at the contact points is measured with accelerometers. For the source mobility measurements, the passive structures are excited by a shaker and the induced force is measured by a force transducer. Similarly, the receiver mobilities are obtained by relating the induced force from the shaker with the velocity response at the contact points. The contact forces are measured by placing force transducers between the source and receiver structures in the installed condition.

The velocity and force orders as well as the interface mobilities are obtained by Eqs. (2)–(4). For the multi-point case, the definition of the velocity and force orders and the interface mobilities can be re-written into a discrete Fourier transform, where the applicability of fast Fourier transform algorithms facilitates short computation times [15].

In order to determine the importance of the cross-order terms for the transmitted power based on the free source velocity, the equal-order approximation from Eq. (9) can be compared with the prediction of the matrix formulation [8]

$$W = \tfrac{1}{2}\mathrm{Re}[\mathbf{v}_{FS}^{\mathrm{T}}(\mathbf{Y}_S+\mathbf{Y}_R)^{-1T}\mathbf{Y}_R^{\mathrm{T}}(\mathbf{Y}_S+\mathbf{Y}_R)^{-1*}\mathbf{v}_{FS}^{*}]. \tag{16}$$

The equal-order approximation of the source descriptor can be obtained from Eq. (12). For comparison, the source descriptor can be calculated by the matrix formulation [8]. As discussed in Section 2, the source descriptor equals the complex power of the free source velocity and the blocked force. In terms of the matrix formulation this yields the characteristic power [7], see Eq. (17). Since Eqs. (10) and (17) are equal, the same symbol is used for the characteristic power as for the source descriptor:

$$S = \tfrac{1}{2}\mathbf{v}_{FS}^{\mathrm{T}}\mathbf{Y}_S^{-1*}\mathbf{v}_{FS}^{*}. \tag{17}$$

For the installations in the present section, the comparison between the equal-order approximation and the matrix formulation contains two uncertainties. For a proper sampling along the interface, the distance between two points has to be smaller than half the governing wavelength [16]. This condition is not fulfilled for the four-point installations under consideration at high frequencies. Hence, an uncertainty is present due to the undersampling at high frequencies. Furthermore, due to conditioning problems in the matrix inversion in the presence of measurement errors [17], the matrix formulation also contains an uncertainty.

If the data available are the contact forces, the complete formulations of the concept of interface mobilities for the transmitted power including the equal-order and cross-order terms can be compared with the equal-order approximation, see Eq. (6). In such a comparison, both predictions are equally undersampled and the difference between the two solely consists of the cross-order terms. Hence, this comparison does not include the aforementioned uncertainties and is expected to yield fully reliable results regarding the importance of the cross-order terms.

Both the predictions from the matrix formulation and the interface mobility approach of the transmitted power are found to yield negative values at certain frequencies. In an installation of an active source structure connected to a passive receiver structure, negative real parts of the power can occur for instance due to the omission of moments and in-plane forces, an air-borne sound excitation of the receiving structure or numerical instabilities. As it is unclear which phenomena apply, the negative values of the transmitted power are omitted in the averaging.

As mentioned above, the source descriptor can be interpreted as the power required to obtain the free source velocity along the interface of the freely suspended source without the internal excitation [2]. Hence, a negative real part of the source descriptor would imply that the passive source emits power, which can be described as unphysical [18]. As for the transmitted power, therefore, negative real parts of the source descriptor are treated as erroneous and consequently are deleted.

7.1. *Installation with rectangular interface and receiving structure with distinctively differing transfer paths*

For an experimental investigation of the conditions outlined and theoretically analyzed in Sections 3 and 4, the source–receiver installation shown in Fig. 21 is selected. The source is a kitchen extractor fan constructed of sheet metal with a rectangular alignment of the connection points with an aspect ratio of 3. A desk is used as receiving structure since it is very similar to kitchen cabinets to which kitchen extractor fans normally are installed. The transfer path on the receiver from the front to the back is substantially shorter than from one side to the other. Owing to divergence and damping, the transfer mobilities of the receiving structure are expected to vary substantially at high frequencies. From the measured data it is found that the transfer mobilities differ from each other by one order of magnitude at frequencies above 500 Hz.

In Fig. 22(a) is plotted the transmitted power calculated by the equal-order approximation based on the free source velocity in comparison with the prediction by the matrix formulation. The complete and relaxed formulation in terms of interface mobilities of the transmitted power based on the contact forces from Eq. (6) are compared in Fig. 22(b). In the respective upper graphs are shown the third-octave band averaged power spectra giving information about the overall magnitude of the data. The three lower graphs in Figs. 22(a) and (b) show the unaveraged transmitted power in three narrow frequency regions, indicating the signature of the data.

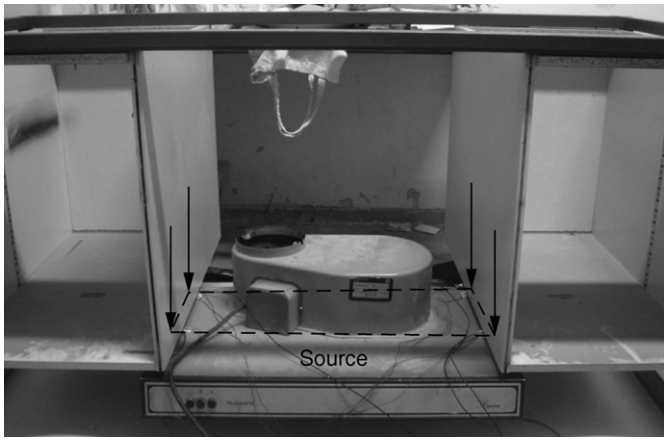

Fig. 21. Installation with rectangular interface and receiving structure with distinctively differing transfer paths. – – – interface; ⟶ contact points.

The matrix formulation and the equal-order estimate of the interface mobility approach based on the free source velocity show a close agreement, particularly at frequencies above 500 Hz. At lower frequencies, larger differences can be observed, where the equal-order approximation both over- and under-estimates the prediction from Eq. (16). It is interesting to note that although only the lowest three orders are included in the approximation in Fig. 22(a), a close agreement occurs even at high frequencies. A matching in both magnitude and signature is seen to be present between the two predictions based on the contact forces. Visible deviations are observed in narrow frequency regions only, e.g. between 60 and 90 Hz.

In Fig. 23, the magnitude of the equal-order approximation of the source descriptor from Eq. (12) is compared with that of the source descriptor calculated by the matrix formulation, see Eq. (17). A high degree of similarity is observed in the overall magnitude as well as the signature of both calculations, particularly at frequencies above 200 Hz.

A significant strengthening of the cross-order terms, particularly at frequencies where the transfer mobilities of the receiver differ substantially, could not be observed. The findings from the theoretical analyses in Sections 3 and 4, therefore, are corroborated by the experimental results.

7.2. Installation with suppressed zero-order motion of the receiving structure and deterministic phase of the contact forces

A suppression of the zero-order motion and a deterministic phase of the contact forces can theoretically lead to a significant strengthening of the cross-order terms, see Sections 5 and 6. For an experimental investigation of these conditions, a simply supported plate is designed as receiving structure and a compact source is chosen which has a distinct and wide mass-controlled frequency region, see Fig. 24.

The compact polishing machine is running at 1400 rpm and has a rectangular interface with an aspect ratio of 1.4. The mass-controlled region of the source mobilities ranges up to approximately 200 Hz. The receiver is an 18 mm thick chipboard plate, supported by semi-circular aluminium profiles, resting on a concrete flag which in turn rests on the concrete floor, see Fig. 24(b). Although the zero-order motion of the receiver is suppressed, the equal-order interface mobility of order zero dominates all other interface mobilities by a factor ranging from 10 to 1. A distinct mass controlled region of the receiver mobilities is found between 10 and 20 Hz, a distinct stiffness-controlled region between 100 and 200 Hz.

In Fig. 25(a), the transmitted power calculated by the matrix formulation is compared with the approximation of the interface mobility approach, see Eqs. (16) and (9), respectively. Due to the numerous negative power values at low frequencies, the matrix formulation fails to capture the peak at the spin frequency of the polishing machine. Apart from this deviation between 20 an 30 Hz, an agreement is observed between both predictions. As for the kitchen extractor fan installation, larger differences occur between the predictions based on the free source velocity than between those based on the contact forces. As shown in Fig. 25(b), a high degree of similarity is observed for the overall magnitude as well as the signature of both predictions based on the contact forces.

The magnitude of the source descriptor from Eqs. (12) and (17) for the compact polishing machine is plotted in Fig. 26. Despite some narrow-band over- and under-estimations, both predictions show a close agreement.

8. Concluding remarks

The applicability of interface mobilities for the characterization of vibrational sources depends on the admissibility of neglecting the cross-order terms. Four conditions are investigated regarding a possible strengthening of the cross-order terms. These are non-circular interface geometries, structures with distinctively differing transfer paths, a suppression of the zero-order motion and a deterministic phase of the contact forces. A strengthening of the cross-order terms due to

non-circular interface geometries or distinctively differing transfer paths is found to be of subordinate significance. Theoretically, the cross-order terms can be strengthened significantly by a suppression of the zero-order motion and a deterministic phase of the contact forces. For practical cases, however, a significant strengthening of the cross-order terms is not observed.

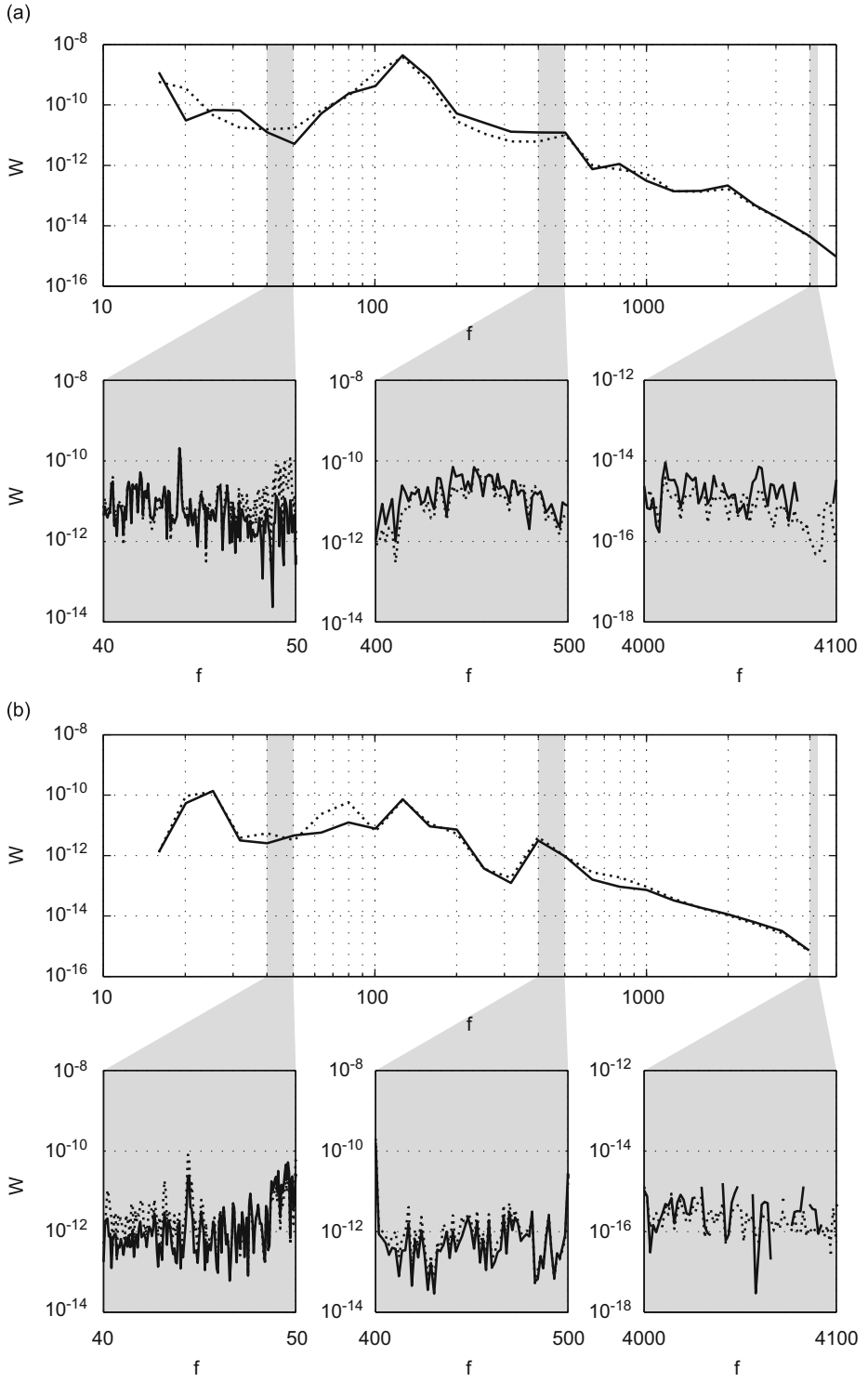

Fig. 22. Third-octave band spectral averaged and narrow band unaveraged transmitted power for an installation with distinctively differing transfer paths: (a) based on the free source velocity; (b) based on the contact forces. —, complete formulation; ···, equal-order approximation.

In accordance with the aforementioned conditions that can possibly lead to a strengthening of the cross-order terms, two potentially critical source–receiver installations are examined. The transmitted power and the source descriptors predicted by the equal-order approximations of the interface mobility approach are compared with the complete calculations. A close agreement is observed for the overall magnitude as well as the signature of the predictions, yielding a good approximation by neglecting the cross-order terms. The theoretical findings and the results from the experimental investigation, therefore, further substantiate the admissibility of neglecting the cross-order terms.

It should be noted, however, that neglecting the cross-order terms can result in large misinterpretations at certain frequencies. On average, however, the cross-order terms are found to be insignificant and can be neglected with good approximation. Hence, the general applicability of interface mobilities for structure-borne sound source characterization and the description of the transmission process is confirmed. The results indicate, moreover, a higher numerical stability for the interface mobility approach than the matrix formulation at low frequencies. It should be mentioned that these indications are based on high quality laboratory data.

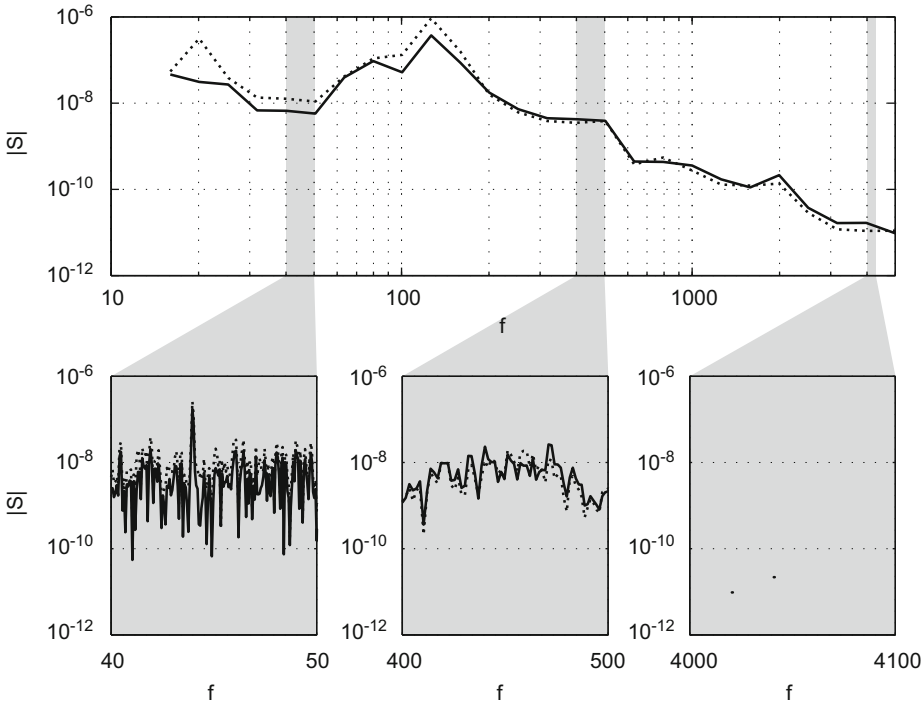

Fig. 23. Third-octave band spectral averaged and narrow band unaveraged source descriptor for an installation with distinctively differing transfer paths. —, matrix formulation; ⋯, equal-order approximation.

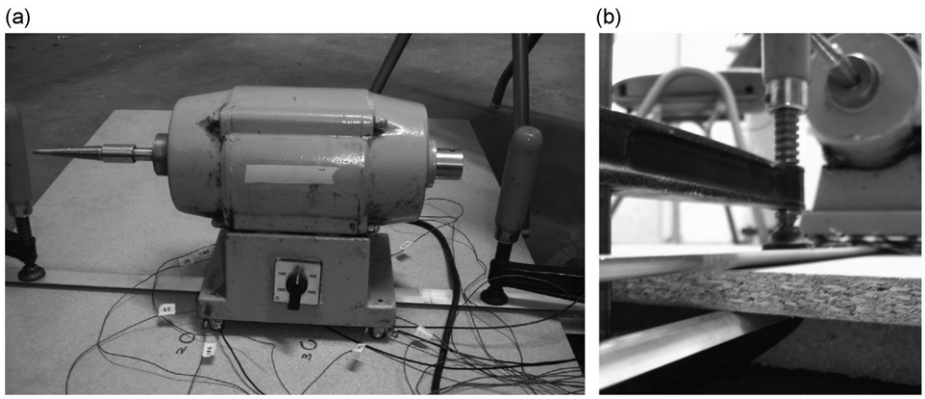

Fig. 24. Compact source installed on a simply supported plate: (a) compact polishing machine; (b) simple support.

With the confirmation of the applicability of interface mobilities for source characterization and the description of the transmission process, the practicability of the approach remains to be investigated. The practicability of the concept of interface mobilities is primarily determined by the number of orders that are required for a proper resolution in the intermediate and upper frequency regions. From the multi-point installations studied in this work, it is observed that

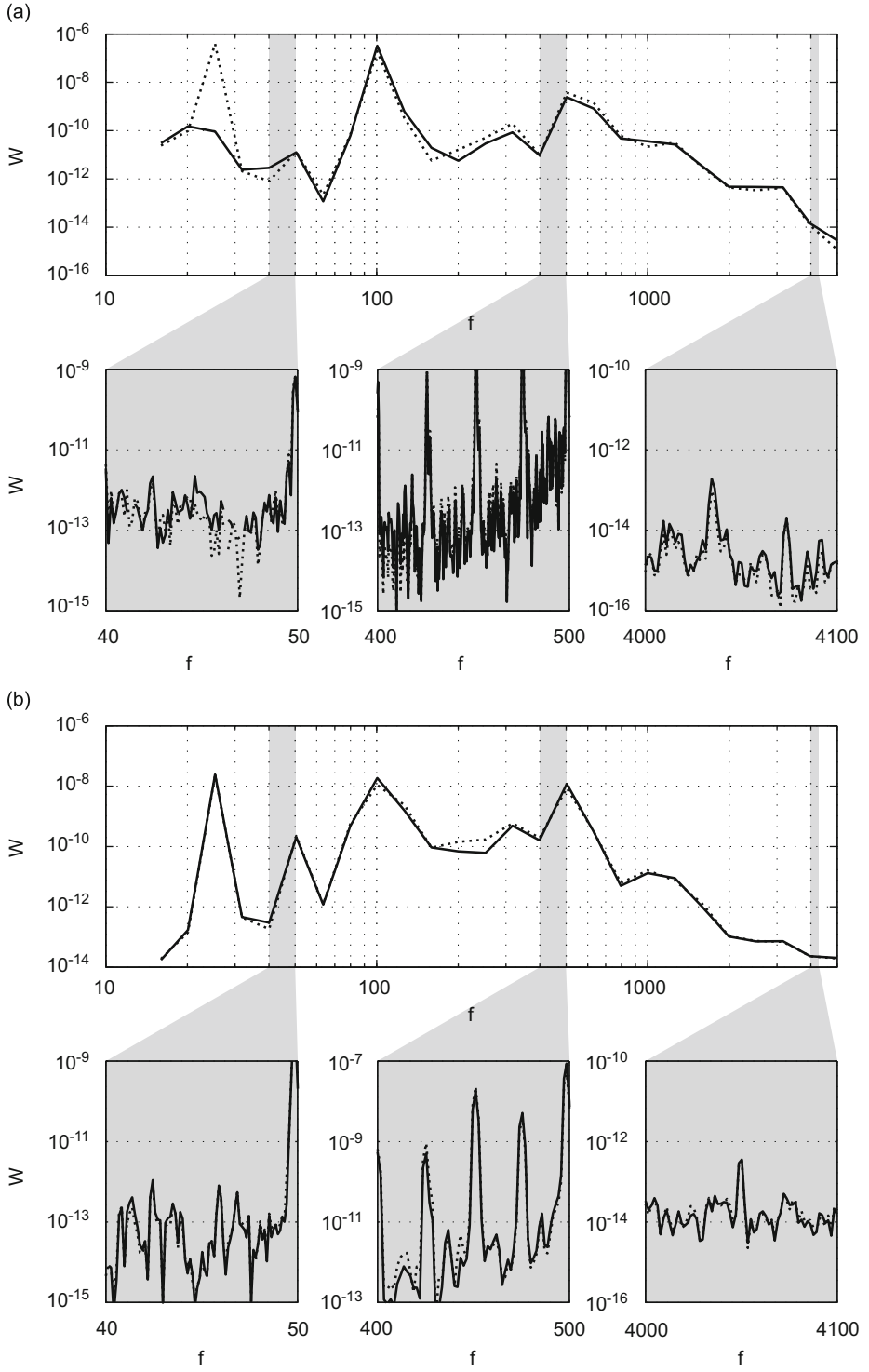

Fig. 25. Third-octave band spectral averaged and narrow band unaveraged transmitted power for a compact source installed on the simple support of a finite plate: (a) based on the free source velocity; (b) based on the contact forces. —, complete formulation; ···, equal-order approximation.

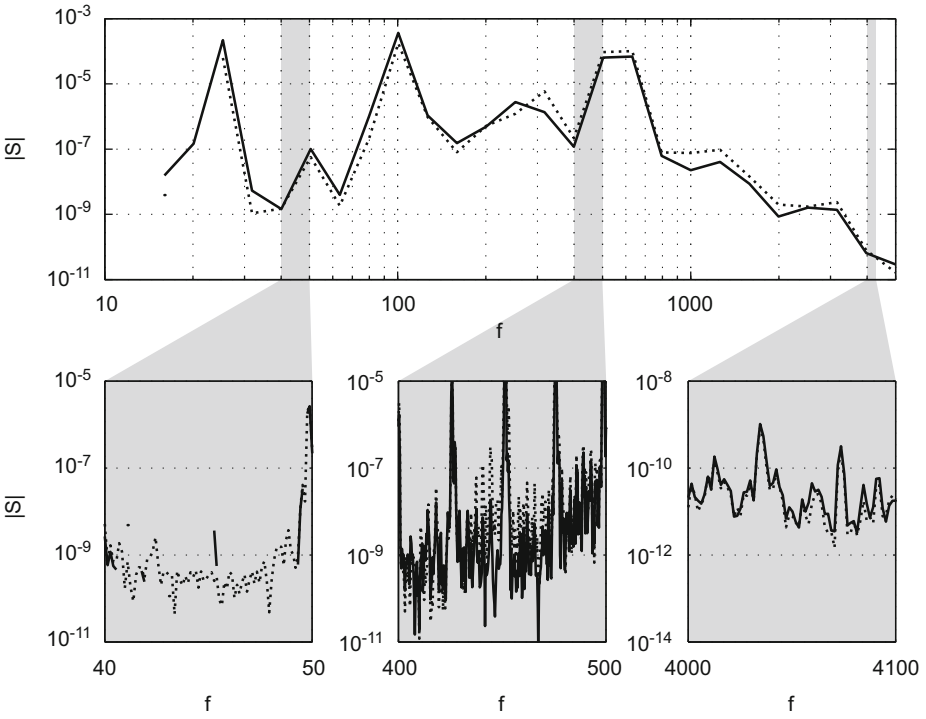

Fig. 26. Third-octave band spectral averaged and narrow band unaveraged source descriptor magnitude for a compact source installed on the simple support of a finite plate. —, matrix formulation; ⋯, equal-order approximation.

the contribution of higher orders than the zero and first orders tend to be insignificant. However, there still is a need for a general clarification of the influence and significance of higher-order terms.

The practicability of the interface mobility approach also depends on the extent of the input variables such as the mobilities and velocities that is required for the calculation of the various orders. In analogy with the Nyquist criterion, it should be possible to obtain the order zero from the data at merely two contact points. In order to reduce the required measurement or simulation work, therefore, the possibility to use reduced data sets could be investigated.

Acknowledgments

The authors gratefully acknowledge the financial support received from the German Research Foundation (DFG) through Grant PE 1155/4-1.

References

[1] B.A.T. Petersson, B.M. Gibbs, Towards a structure-borne sound source characterization, *Applied Acoustics* 61 (2000) 325–343.
[2] J.-M. Mondot, B.A.T. Petersson, Characterization of structure-borne sound sources: the source descriptor and the coupling function, *Journal of Sound and Vibration* 114 (1987) 507–518.
[3] H.A. Bonhoff, B.A.T. Petersson, The influence of cross-order terms in interface mobilities for structure-borne sound source characterization: plate-like structures, *Journal of Sound and Vibration* 311 (2008) 473–484.
[4] H.A. Bonhoff, B.A.T. Petersson, The influence of cross-order terms in interface mobilities for structure-borne sound source characterization: frame-like structures, *Journal of Sound and Vibration* 319 (2009) 305–319.
[5] H.A. Bonhoff, B.A.T. Petersson, The influence of cross-order terms in interface mobilities for structure-borne sound source characterization: force-order distribution, *Journal of Sound and Vibration* 322 (2009) 241–254.
[6] B.A.T. Petersson, B.M. Gibbs, Use of the source descriptor concept in studies of multi-point and multi-directional vibrational sources, *Journal of Sound and Vibration* 168 (1993) 157–167.
[7] A.T. Moorhouse, On the characteristic power of structure-borne sound sources, *Journal of Sound and Vibration* 248 (2001) 441–459.
[8] L. Cremer, M. Heckl, B.A.T. Petersson, *Structure-borne Sound*, third ed., Springer-Verlag, Berlin, 2005.
[9] B.A.T. Petersson, Structural acoustic power transmission by point moment and force excitation, Part 2: plate-like structures, *Journal of Sound and Vibration* 160 (1993) 67–91.
[10] M. Heckl, Structure-borne sound propagation on beams with many discontinuities, *Acustica* 81 (1995) 439–449.
[11] R.A. Fulford, B.M. Gibbs, Structure-borne sound power and source characterization in multi-point-connected systems, Part 2: about mobility functions and free velocities, *Journal of Sound and Vibration* 220 (1999) 203–224.
[12] R.A. Fulford, B.M. Gibbs, Structure-borne sound power and source characterization in multi-point-connected systems, Part 3: force ratio estimates, *Journal of Sound and Vibration* 225 (1999) 239–282.
[13] C.M. Harris, A.G. Piersol, *Harris' Shock and Vibration Handbook*, fifth ed., McGraw-Hill, 2002.

[14] M.C. Junger, D. Feit, *Sound, Structures, and their Interaction*, MIT Press, New York, 1986.
[15] H.A. Bonhoff, The influence and significance of cross-order terms in interface mobilities for structure-borne sound source characterization, Ph.D. Thesis, Institute of Fluid Mechanics and Engineering Acoustics, Technische Universität Berlin, Germany, 2009.
[16] B.A.T. Petersson, An experimental technique for dynamic characteristics at large structural interfaces, *International Congress on Sound and Vibration*, Vol. 6, Copenhagen, Denmark, 1999, pp. 2175–2182.
[17] G. Pavic, *Noise sources and noise synthesis*. Inter-Noise, 08, 2008, Shanghai, China.
[18] A.T. Moorhouse, B.M. Gibbs, Measurement of the characteristic power of structure-borne sound sources, *International Congress on Sound and Vibration*, Vol. 6, Copenhagen, Denmark, 1999, pp. 2161–2168.